Egyptian Journal of Cell and Tissue Research
Print ISSN: 2812-5436 / Online ISSN: 2812-5444

Possible Protective Effect of Co-administration of Hydrogen Sulfide and Exosomes versus Hydrogen Sulfide Preconditioned Exosomes on Hepatic Ischemia Reperfusion Injury in Adult Male Rat Model: Biochemical, Histological and Immunohistochemical Study

Marwa Mohamed Yousry, * Dalia Fathy Abdelmaksoud El-Deeb *, Esraa Samy Abd El-Sattar *, Wafaa Abd El-Azeem Abdou Boughdady *

*Histology Department, Faculty of Medicine, Cairo University, Cairo, Egypt**

Abstract:

Background: Liver ischemia/reperfusion (I/R) commonly happens within liver surgical procedures as well as transplantation. It causes postoperative liver dysfunction, and poor patient outcome. Emerging strategies assume that efficacy of mesenchymal stem cells-exosomes (MSCs-EXOs) is dependent on status of MSCs extracellular environment. Hydrogen sulfide (H_2S) regulates several cellular signaling pathways and exerts a protective effect in various disorders. **Aim of the work:** Comparing the protective influence of co-administration of H_2S and exosomes versus H_2S-preconditioned exosomes on liver I/R injury adult male rat model. **Materials and Methods:** Fifty adult male rats were categorized to donor, control, liver I/R, recovery, H_2S + EXOs, and H_2S-preconditioned EXOs groups. At the end of experiment, biochemical analysis [for liver enzymes, nuclear factor kappa-B (NF-κB) and superoxide dismutase (SOD)], histological and immunohistochemical studies [for high-mobility group box 1 (HMGB1), nuclear factor-erythroid 2-related factor 2 **(**Nrf2), as well as heme oxygenase-1 **(**HO-1)], and statistical analysis were done. **Results:** Ischemia/reperfusion group recorded significant rise in hepatic enzymes, NF-κB level, HMGB1 immunoreactivity, and decrease in SOD level, Nrf2 and HO-1 immunoreactivity. In addition to the presence of foci of disorganized hepatocytes, necrotic cells, apoptosis, and periportal inflammatory infiltration. Recovery showed insignificant improvement in formerly mentioned results. While the use of H_2S + EXOs, or H_2S-

precoordinated EXOs clearly improved inflammation, antioxidant parameters, and hepatocellular injury. **Conclusion:** H_2S + EXOs in addition to H_2S-precoordinated EXOs possessed hepatoprotective impacts against I/R injury in the liver. Whereas H_2S preconditioning of MSCs could augment the protective impact of MSC-EXOs.

Keywords: Hepatic I/R injury, EXOs+ H_2S, H_2S Preconditioned EXOs, HMGB1, Nrf2/HO1.

1. Introduction:

Hepatic ischemia reperfusion injury (HIRI) is a critical consequence of multiple operative procedures as in resection as well as transplantation of liver [1]. Liver I/R stimulates inflammatory along with immunological responses that may result in liver dysfunction and acute or chronic rejection of graft in cases of hepatic transplantation. This could affect the prognosis of recipient [2]. Thus, it is critical for successful liver transplantation surgery to avoid hepatic I/R [3].

During the period of ischemia, loss of the arterial supply leads to disturbed balance between metabolic supplements and needs, creating a hypoxic status in liver tissues. Moreover, during reperfusion period, the return of blood flow triggers aggravated inflammatory reaction in addition to oxidative stress [4]. These series of events occurring during I/R causes reactive oxygen species (ROS) to accumulate in hepatic tissues, inducing severe hepatocellular injury [5].

High-mobility group box 1 (HMGB1) is a pro-inflammatory factor, a key trigger of inflammatory reaction during I/R of liver. HMGB1 release is mediated through the production of ROS following liver ischemia. Therefore, the antioxidant approach for suppressing release of HMGB1 may have a hopeful effect in the protection as well as management of liver I/R [6].

Nuclear factor-erythroid 2-related factor 2 (Nrf2)/ heme oxygenase-1 (HO-1), a necessary antioxidant signaling pathway, maintain homeostasis of redox state for protection against cellular oxidative stress [7]. During physiological status, Nrf2 in addition to its negative regulator Kelch-like epichlorohydrin (ECH)-associated protein 1 (Keap1) are present in cytoplasm. During stressful situations, Nrf2 dissociates from Keap1, allowing translocation of Nrf2 to the

nucleus then interact with antioxidant response element (ARE), key antioxidant pathway [8]. ARE genes is comprising antioxidant enzymes, such as superoxide dismutase (SOD), catalase (CAT), glutathione peroxidase (GPx) as well as glutathione-S transferase (GST), anti-inflammatory proteins, heme oxygenase-1 (HO-1), and cyclooxygenase-2 (COX-2) [9, 10]. HO-1, an initial antioxidant enzyme related to ARE genes, involved in defense process against liver oxidative injury. Upon activation it leads to redox homeostatic balance, inhibition of inflammatory responses and suppression of tissue damage [11]. The Nrf2/ARE pathway exhibits a major effect in defense against liver I/R injury [12].

Stem cells therapy is a new strategy that allows management of various diseases and injuries. Whereas the implanted stem cells have poor survival rate especially in hypoxic status leading to ineffective therapeutic action [13,14].

To overcome such obstacles, exosomes have appeared as a target to attain better therapeutic results with extended circulatory life. Exosomes, lipid bi-layer cellular vesicles, are secreted for intercellular signaling [15]. Exosomes are a substantial paracrine element for stem cells [16]. They have a prominent effect in regeneration of affected organs through promotion of cell-to-cell connection [17]. Exosomes transport their cargo lipids, proteins, also nucleic acids to the target cells, influencing various signaling and biological processes inside the target cells [18].

Modification of MSCs media may enhance their effects by changing the secreted paracrine factors [19]. Various methods of preconditioning of MSCs have been tested, comprising preconditioning with pharmacological/chemical, hypoxia preconditioning, physical elements, trophic factors, or cytokines preconditioning [20].

Hydrogen sulfide (H_2S) is one of the endogenously synthesized gaseous molecules with major cytoprotective effects against cell injury and death. This is mediated via combating reactive oxygen and nitrogen species [21,22]. Among the different donors of hydrogen sulfide, sodium hydrogen sulfide (NaHS); is commonly used as a fast-releasing hydrogen sulfide donor both in-vivo as well as in-vitro [23].

This work aimed at comparing the protective influence of co-administration of H_2S (liberated from sodium hydrogen sulfide) and exosomes versus H_2S preconditioned exosomes on liver I/R injury in adult male albino rat.

2. Material and methods:

A- Materials:

Drugs:

1- Sodium hydrosulfide (NaHS):

A H_2S donor was obtained from Sigma-Aldrich chemical company, USA in the form of chips which were crushed and dissolved in normal saline [24]. It was prepared at concentration of 11.2 µmol/ml saline for rat administration and 200 µmol/L phosphate buffer saline (PBS) for adipose tissue mesenchymal stem cells (AMSCs) pretreatment. These preparations were performed at Biochemistry Department, Faculty of Medicine, Cairo University.

2- Paul Karl Horan-26 (PKH-26) labelled adipose tissue mesenchymal stem cells derived exosomes (AMSCs-EXOs):

Preparation and isolation of exosomes from AMSCs conditioned media was obtained via ultracentrifugation according to ***Yuan et al., 2019*** [25] methodology. Exosomes were extracted from AMSCs and labeled with PKH-26 dye (Sigma-Aldrich chemical company, USA) to trace homing of exosomes in the liver tissues.

Exosomes were provided as 100µg EXOs/100µl of PBS.

3- H_2S preconditioned AMSCs derived exosomes (H_2S preconditioned AMSCs-EXOs):

AMSCs were pretreated with 200 µmol/L NaHS for 30 minutes followed by EXOs collection. Subsequently exosomes were labelled with PKH-26 and provided as 100µg EXOs/100µl PBS [26].

AMSCs preparation and pretreatment along with exosomes preparation, isolation, collection and labelling were achieved at Histology Department, Faculty of Medicine, Cairo University

Animals:

The current work included 50 male albino rats, approximately 12 weeks age, 200 grams weight. The animals were maintained in the animal house of Faculty of Medicine, Cairo University and were handled respective to instructions approved by Cairo University-Institutional Animal Care and Use Committee (CU-IACUC) [approval number CU/III/F/46/23]. They were maintained in cages under standard environmental state (at 24 ± 1°C in normal light/dark cycle) & allowed access to chow along with water *ad libitum* for 2 days former to the onset of study to acclimate to the environmental circumstances. Then the animals were kept in previous situations through the entire experimental durations.

Experimental Design

Donor group:

Two rats were applied for AMSCs isolation, culturing, phenotyping, as well as extraction of exosomes.

The remaining 48 rats were categorized into 5 groups:

Group I (Control group) (8 rats): was subdivided equally in 4 subgroups (2 rats each), rats did not undergo the procedure of ischemia/reperfusion injury:

- **Subgroup Ia:** animals were not subjected to any procedures or treatments, serving as negative control.
- **Subgroup Ib:** sham rats were submitted to laparotomy only without cross clamping the bilio-vascular pedicle, sacrificed corresponding to group II (I/R group) & III (Recovery group).
- **Subgroup Ic:** rats were operated as subgroup Ib and each animal was injected intraperitoneally (IP) in the lower right quadrant with 1ml saline concomitantly with portal vein injection of a 100 µl PBS, corresponding to group IV (H_2S + EXOs).
- **Subgroup Id:** rats were operated as subgroup Ib and each rat was injected once intravenously (IV) via the portal vein with a 100 µl PBS, corresponding to group V (H_2S preconditioned EXOs).

Group II (I/R group) (10 rats):

Anesthesia of rats was performed by ketamine intramuscular injection (50 mg/kg) [27] followed by transverse abdominal incision to access liver [28]. Then, the hepatic artery, common bile duct, along with portal vein, which make up the hepatic vascular pedicle of whole liver was clamped by microvascular bulldog clamp**.** After thirty minutes of total hepatic ischemia (THI), removal of clamp was done to start hepatic blood flow. After that, suturing of the abdomen was accomplished in 2 layers by 4-0 continuous sutures (Vicryl 4-0; Ethicon) and rats were sacrificed after 2 hours of reperfusion [29].

Group III (Recovery group) (10 rats):

Rats underwent I/R as in group II and were injected subcutaneously with buprenorphine (0.03 mg/kg/24 hour) in addition to cefuroxime sodium (16 mg/kg/24 hour) (Sigma-Aldrich chemical business, Cairo, Egypt) as analgesia and antibiotic treatment. Animals were closely monitored for the first four hours following surgery before being returned to their cages [29]. Then they were sacrificed 48 hours after reperfusion.

Group IV (H_2S and exosomes) (H_2S + EXOs) (10 rats):

Rats were subjected to laparotomy as in group II and each rat was injected IP at lower right quadrant (to avoid spilling of the drug) with a single dose of 11.2 µmol NaHS dissolved in 1ml saline (56 µmol/kg NaHS)

[28] concomitantly with a single IV injection of 100 µg exosomes suspended in 100 µl PBS [26] through portal vein [30]. Then rats were immediately subjected to I/R as in group II.

Group V (H_2S preconditioned exosomes group) (H_2S preconditioned EXOs) (10 rats):

Rats were subjected to laparotomy as in group II and each animal was injected once via the portal vein with a 100 µl PBS containing 100 µg exosomes of AMSCs preconditioned with 200 µmol/L NaHS [26] then I/R was conducted in rats as in group II animals.

B- Methods

ADMSCs and Exosomes Study:

Preparation, isolation, and collection of AMSCs derived exosomes:

A. Preparation of AMSCs:

For isolation of the AMSCs, digestion of 5 g of abdominal adipose tissue from the 2 donor rats was applied in Dulbecco's Modified Eagle Medium (DMEM) (Cat. No. 12491015, Gibco, UK) having collagenase type I (CAS 9001-12-1, Sigma Aldrich, USA) at 37°C for 2 hours on a shaker. The resultant suspension underwent a 10-minute centrifugation at 1,200 g. After centrifuging, the supernatant was drained off, the pellet was returned to DMEM having 10% (volume/volume) fetal bovine serum (FBS) as well as 1% (volume/volume) penicillin/streptomycin until about 80% confluency (~1 × 10^6 cells) with 2 passages was obtained [31].

Examination of unconditioned AMSCs and H_2S preconditioned AMSCs using cell proliferation assay:

The cell proliferation assay of the unconditioned AMSCs and H_2S preconditioned AMSCs pretreatment with 200 µmol/L NaHS for 30 minutes [26] was done at the Biochemistry Department, Faculty of Medicine, Cairo University as follows: A cell proliferation kit (Trevigen Inc., USA) was used to measure the proliferation of untreated AMSCs and AMSCs preconditioned with NaHS in accordance with the guidelines of manufacturer instructions.

B. Exosomes and H_2S preconditioned EXOs collection and purification:

According to ***González-Cubero et al., 2021*** study [31]; for collection of AMSCs-derived exosomes, serum-free DMEM with 1% penicillin/streptomycin was added to the cells to prevent any contamination. Then supernatants were obtained from the AMSCs-conditioned medium after 24 hours. Whereas, for collection of H_2S preconditioned exosomes, AMSCs were

pretreated with 200 µmol/L NaHS for 30 minutes followed by exosomes collection [26].

For exosomes purification of either non-NaHS treated or NaHS-treated AMSCs, centrifugation was performed on the obtained culture supernatants at 300 g in addition to 2,000 g for ten minutes individually at 4 °C. After that, the supernatant underwent a centrifugation process at 10,000 g for thirty minutes at 4 °C for elimination of large sized particles. Then centrifugation of exosomes at 100,000 g for seventy minutes at 4°C to pellet them. Then, the pellet was rinsed with PBS (Product No. P5368, Sigma Aldrich, USA), followed by centrifugation once more at 100,000 g for 70 minutes at 4°C [31].

Identification of exosomes:

A-Examination of exosomes and H_2S preconditioned EXOs by transmission electron microscope (TEM):

Exosomes and H_2S preconditioned exosomes were examined at the Electron Microscope Research Unit, Faculty of Agriculture, Cairo University (**Figs. 1a &1b)**. Exosomes appeared as spherical shaped vesicles with variable diameter, average 75 nm. According to ***Willis et al., 2018*** [32]; exosomes were identified with spherical morphology under TEM with diameter of 30-150 nm**.**

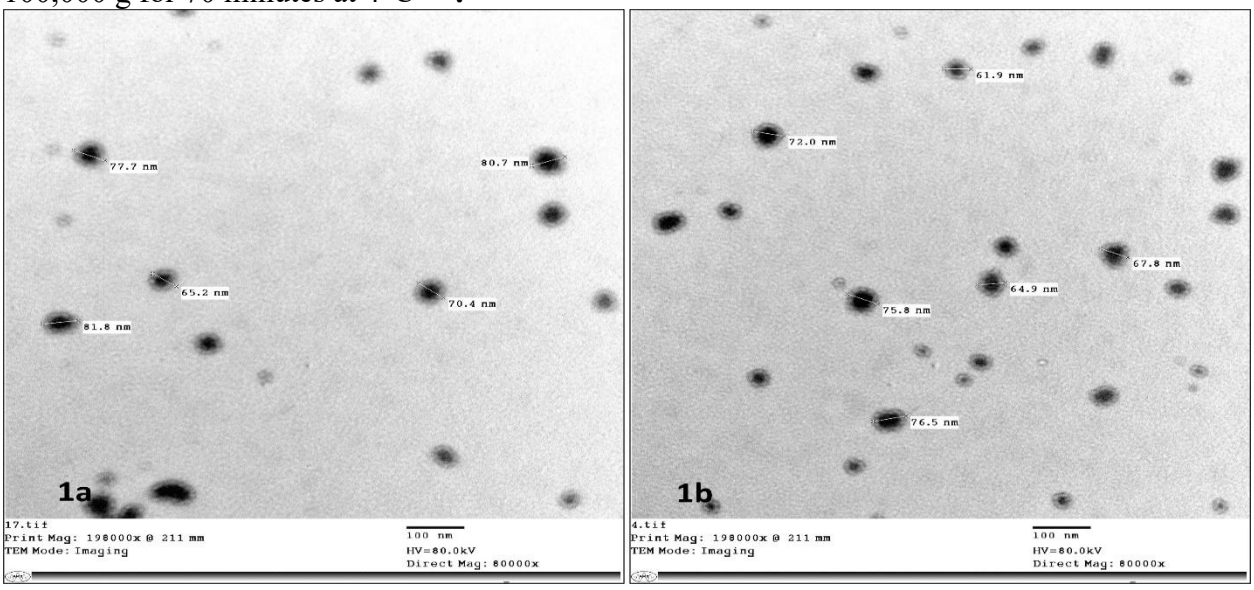

Figure 1: TEM photomicrographs showing EXOs with an average diameter of 75 nm of both **1a:** ADMSCs-unconditioned EXOs. **1b:** H_2S preconditioned ADMSCs-EXOs.

[x 80000].

B -Total protein content using Bradford assay:

According to ***Hajian et al., 2021*** [33]; total content of proteins was estimated by Bradford assay (Quick Start Kit, Bio-Rad) respective to manufacturer's datasheet. This test was performed at the Biochemistry Department, Faculty of Medicine, Cairo University.

III. Labeling of exosomes:

The exosomes were stained with PKH-26 using PKH-26 red fluorescent dye (Cat. No. MIN126, Sigma, USA) for their labeling.

Animal studies:

I. Biochemical studies

Samples of blood were collected from rats of groups (I, II, IV & V) at the end of the 2 hours reperfusion duration, just before sacrifice. Whereas they were collected from rats of group (III) after 48 hours reperfusion. Butterfly needles were used to collect them from tail vein [34]. Blood samples were tested for alanine aminotransferase (ALT) as well as aspartate aminotransferase (AST) by colorimetric method in accordance to manufacture instructions of BioAssay Systems Company (California, USA).

Rats of groups (I, II, III, IV & V) were euthanized by ketamine IP injection (80 mg/ kg) and xylazine (10 mg/kg) [35]. Liver specimens from rat's median lobe of control and all experimental groups were collected and divided into two specimens, the first specimen for tissue biochemical analysis and the second specimen for histological studies.

The first specimen was for biochemical analysis of tissue nuclear factor kappa B (NF-κB) level, a regulator of proinflammatory cytokines, has a significant impact in liver I/R inflammatory reaction, [36] and superoxide dismutase level (SOD) an antioxidant enzyme that has a major effect in defense mechanism against ROS activities [37]. NF-κB and SOD were analyzed via the corresponding enzyme-linked immunosorbent assay (ELISA) kits (MBS287521 and MBS036924 respectively, MyBioSource; USA).

Biochemical analysis of serum ALT & AST and tissue NF-κB & SOD levels was evaluated at the Biochemistry Department, Faculty of Medicine, Cairo University.

II. Histological studies:

All studies were accomplished at the Histology Department, Faculty of Medicine, Cairo University. Fixation of liver specimens in 10% formol saline was followed by processing of paraffin block.

Six µm thick serial sections were sliced for the following studies:

i. Fluorescent microscopic study: unstained sections of groups I (as a negative group), IV and V (to detect homing of exosomes) were examined by fluorescent microscope Olympus BX50F4.

ii. Light microscopic study:

1- Hematoxylin and Eosin (H&E) stain [38]. To demonstrate histological structure and alterations of liver.

2- Immunohistochemical staining for [38] for:

High-mobility group box 1 (HMGB1): is a rabbit polyclonal antibody (A2553, ABclonal Boston, MA, USA) that appears in the nucleus. HMGB1 is an essential inflammatory cytokine during I/R injury, that promotes inflammatory responses as well as stimulates cell apoptosis [39].

Nuclear factor-erythroid 2-related factor 2 (Nrf2): is a rabbit polyclonal antibody (A11159, ABclonal Boston, MA, USA) that appears in the cytoplasm. Nrf2, a main transcription factor for controlling the cellular oxidative stress, can regulate primary defense processes against ROS-induced tissue injury [40].

Heme oxygenase-1 (HO-1): is a rabbit polyclonal antibody (A1346, ABclonal Boston, MA, USA) that appears as cytoplasmic reaction. HO-1 is a Nrf2-regulated gene, upregulation of its expression is a cytoprotective mechanism against cellular stresses [41].

- Immunostaining was carried out using avidin-biotin technique [38] by:

1- Antigen retrieval, liver sections were boiled in 10 mM citrate buffer (Cat No. 005000) pH 6 for 10 minutes.

2- Followed by cooling the liver sections for twenty minutes at room temperature.

3-Then incubation of sections with the primary antibodies for 60 minutes was performed. Corresponding to manufacturer's datasheet, the optimal dilution was 1:50 - 1:200 for HMGB1, Nrf2 and HO-1 antibodies.

4-Staining was done using Ultravision One Detection System (Cat No. TL - 060- HLJ) and Lab Vision Mayer's hematoxylin counterstaining (Cat No. TA- 060- MH).

The following were brought from Labvision, ThermoFisher scientific, USA: Citrate buffer, Ultravision One Detection System in addition to Ultravision Mayer's hematoxylin.

HMGB1 positive control showed brown nuclear expression in brain tissue. The positive control for Nrf2 and HO-1

appeared as brown cytoplasmic reaction in brain tissue and liver respectively. Whereas the negative control liver sections were obtained by the former method without addition of the primary antibodies.

III-Morphometric study:

This was accomplished using Leica Qwin 500 LTD image analyzer (Cambridge, England) attached to a light microscope with a colored video camera, for detection of area percent of positive immunoreaction for HMGB1, Nrf2 and HO-1. It was done for six sections from six animals of each group immune-stained with HMGB1, Nrf2 and HO-1 separately. From every section, ten non overlapping microscopic fields were randomly inspected at magnification x 400 using the binary mode.

The count of homed PKH26 labelled AMSCs derived exosomes (×400) was analyzed in ten non overlapping liver fields using Image J Program.

IV-Statistical analysis:

The obtained data were analyzed through statistical package for social sciences (SPSS) program version 16 (IBM, Armonk. NY, USA). Measurements were summarized as mean and standard deviation (mean ± SD) and compared via one way analysis of variance test followed by "Tukey" post hoc test for all measurements except for cell proliferation assay, total protein quantification assay and number of homed exosomes in liver tissues, an independent samples T-test was used. Probability P values <0.05 appeared significant [42].

3. Results:

ADMSCs & Exosomes Study Results:

I. ADMSCs proliferation assay results:

Cell proliferation of ADMSCs preconditioned with NaHS was 115.28±0.94 and revealed a significant increase in cell proliferation percentile as compared to unconditioned ADMSCs value (98.71±1.25).

II. Exosomes total protein quantification test results:

The mean level of total protein quantification test was 132.67±1.54 and 58.3±1.17 µg/ml in NaHS preconditioned exosomes and unconditioned exosomes respectively. Statistically, this indicated a significant rise in NaHS preconditioned exosomes as compared to unconditioned exosomes.

General observations

- Gross appearance of liver: Before ischemia the liver surface showed no abnormalities **(Fig. 2a).** While after thirty minutes of ischemia, the liver appeared pale **(Fig. 2b).** Two hours after reperfusion,

the liver surface became brown and congested **(Fig. 2c).**

- Deaths were observed in two rats of group II (I/R group) following 1 hour of reperfusion. Regarding rats of group III (recovery group), 4 rats died between 32-36 hours after reperfusion.
- Rats of subgroups Ia, Ib, Ic and Id displayed similar biochemical results, likewise histological findings. So, all of them were considered as a control group (group I).

Serological and tissue homogenates results:

The mean values of serum ALT and AST **(Fig. 3a)** in addition to tissue NF-κB **(Fig.3b)** recorded significant rise in group II (I/R group), group III (Recovery) and group IV (H_2S + EXOs), and non-significant increase in group V (H_2S preconditioned EXOs) versus group I (Control group). Additionally, a non-significant reduction was reported in the recovery group versus I/R group. However, groups IV as well as V detected a significant reduction versus I/R group. Moreover, a significant diminution in group V versus group IV was recorded.

The mean value of tissue SOD level **(Fig.3b)** showed significant low values in all studied groups versus control group except in group V that demonstrated non-significant low values versus group I. Compared to I/R group a non-significant elevation in group III also a significant elevation in groups IV and V were reported. Additionally, a significant elevation was noticed in group V in relation to group IV.

Histological results

I. PKH26 labelled immunofluorescent sections:

Unstained liver sections of groups I (as a negative group) **(Fig.4a)** showed absence of red fluorescence of PKH-26 dye. While PKH-26 labelled EXOs was illustrated inside blood sinusoids in group IV **(Fig.4b)** and inside hepatic blood vessels and blood sinusoids in group V **(Fig.4c)**.

II. Hematoxylin and Eosin-stained sections:

Control group (Figs.5a,5b&5c):

H&E-stained sections illustrated normal hepatic parenchyma with preserved hepatic lobular architecture. Hepatocytes were arranged in plates radiating from the central vein to the periphery of lobule where portal tracts were noticed. The portal tract has a branch of portal vein, hepatic artery, bile duct in addition to a lymphatic vessel. Blood sinusoids were noticed separating

cords of hepatocytes and were lined by endothelial cells along with Kupffer cells. In addition, polyhedral hepatocytes exhibited acidophilic vacuolated cytoplasm as well as central rounded pale nuclei with prominent nucleoli. Some hepatocytes showed binucleation.

Group II (I/R group) (Figs. 5d,5e,5f&5g):

Examination of liver section showed patchy and variable lesion with markedly congested central vein, dilated congested blood sinusoids and distorted hepatic cords. In the pericentral area, hepatocytes were swollen with dark eccentric nuclei and large cytoplasmic vacuolations, others had deeply acidophilic cytoplasm with pyknotic nuclei. Some hepatocytes appeared disfigured with many cytoplasmic vacuolation and eccentric nuclei. As regards the periportal area, there was recruitment of heavy inflammatory infiltration around the portal tract. Foci of markedly disorganized hepatocytes were noticed and surrounded by shrunken hepatocytes with deeply acidophilic cytoplasm and either pyknotic nuclei or fragmented nuclei. Kupffer cells were frequently noted among the sinusoids in pericentral and periportal areas.

Group III (Recovery group) (Figs. 6a,6b,6c,6d &6e):

This group showed histological changes nearly like that of I/R group. Some fields revealed dilated central vein along with dilated sinusoids. Some pericentral hepatocytes showed deeply acidophilic cytoplasm with shrunken darkly stained irregular nuclei. Whereas hepatocytes with multiple cytoplasmic vacuolations were frequently seen in other fields. At the portal tract, areas of deranged hepatocytes close to foci of inflammatory cellular infiltration were noted. Some periportal hepatocytes appeared shrunken containing pyknotic nuclei in addition to deeply acidophilic cytoplasm. Additionally, there were acidophilic cytoplasmic remnants admixed with very small nuclear debris in periportal area. Kupffer cells were frequently noted.

Group IV (H_2S + EXOs) (Figs. 7a,7b&7c):

Examination of liver sections of H_2S + EXOs treated rats illustrated congested central vein, some dilated congested sinusoids, and few inflammatory cells around congested portal tract vessels. Hepatocytes exhibited acidophilic cytoplasm with vesicular nuclei. Some pericentral hepatocytes showed large cytoplasmic vacuolations. Moreover,

periportal liver cells with pyknotic nuclei and deeply acidophilic cytoplasm were seen. Kupffer cells were noted inside the blood sinusoids.

Group V (H_2S preconditioned EXOs) (Figs. 7d,7e&7f):

The liver sections revealed an apparent normal histological architecture of liver lobules. Plates of hepatocytes were seen extending from central vein toward portal tract where few inflammatory cells were noticed. Liver plates were separated by sinusoids containing Kupffer cells. Hepatocytes exhibited central single rounded pale nuclei along with acidophilic cytoplasm. Also, there were some binucleated hepatocytes.

HMGB1 immunostained sections:

The negative control liver sections **(Fig. 8a)** without adding the HMGB1 primary antibody showed negative immunostaining.

Control group (Fig.8b):

Positive HMGB1 nuclear immunostaining was illustrated in hepatocytes, endothelial cells as well as Kupffer cells lining the blood sinusoids**.**

Group II (I/R group) (Fig.8c):

There was positive nuclear immunoreaction in some hepatocytes, endothelial, in addition to Kupffer cells. Also, there was positive cytoplasmic immunoreaction in many hepatocytes and in liver sinusoidal endothelial cells (LSECs).

Group III (Recovery group) (Fig.8d)

Positive cytoplasmic immunoreaction in many hepatocytes along with the presence of cytoplasmic immunoreaction in LSECs were illustrated. Additionally, there was positive nuclear immunoreaction in multiple hepatocytes and in endothelial and Kupffer cells lining the hepatic sinusoids.

Group IV (H_2S + EXOs) (Fig.8e):

Most hepatocytes illustrated positive nuclear immunoreaction. Others showed positive cytoplasmic immunoreaction. Positive immunoreaction in the nuclei and cytoplasm of endothelial cells lining blood sinusoids was demonstrated. In addition, a positive nuclear immunoreaction appeared in Kupffer cells.

Group V (H_2S preconditioned EXOs) (Fig.8f):

Positive HMGB1 nuclear immunoreactivity was seen in multiple hepatocytes. Minimal cytoplasmic immunoreaction appeared in a few hepatocytes. Endothelial cells of blood sinusoids showed positive nuclear and cytoplasmic immunoreactions. In addition,

to the noticed positive nuclear immunoreaction in Kupffer cell.

Nrf2 immunostained sections:

The negative control hepatic sections **(Fig. 9a)** illustrated negative immunostaining when skipping the step of Nrf2 primary antibody**.**

Control group (Fig.9b):

Examination of Nrf2 immuno-stained sections demonstrated positive immunoreactivity in the cytoplasm of hepatocytes.

Group II (I/R group) (Fig.9c):

Liver sections exhibited some hepatocytes with apparently increased positive cytoplasmic immunoreaction when compared to group I. In addition, positive nuclear immunoreaction appeared in a few hepatocytes.

Group III (Recovery group) (Fig.9d)

This group demonstrated some hepatocytes with positive cytoplasmic immunoreactivity as compared to group I. Also, there were few hepatocytes with positive nuclear immunoreactivity.

Group IV (H_2S + EXOs) (Fig.9e):

Many hepatocytes showed positive cytoplasmic immunoreactivity to Nrf2. Additionally, there was positive nuclear immunoreaction in some hepatocytes.

Group V (H_2S preconditioned EXOs) (Fig.9f):

Widely distributed positive cytoplasmic and nuclear immunoreactivity to Nrf2 in most hepatocytes was observed.

HO-1 immunostained sections:

The negative control liver sections **(Fig. 10a)** after skipping HO-1 primary antibody demonstrated negative immunoreaction.

Control group (Fig.10b):

Liver sections illustrated few hepatocytes with positive cytoplasmic immunoreactivity to HO-1.

Group II (I/R group) (Fig.10c):

Positive HO-1 cytoplasmic immunoreaction was demonstrated in some hepatocytes as compared to group I.

Group III (Recovery group) (Fig.10d)

There was positive HO-1 immunoreaction in the cytoplasm of some hepatocytes as compared to control group.

Group IV (H_2S + EXOs) (Fig.10e):

The positive cytoplasmic HO-1 immunoreactivity was noticed in most of hepatocytes.

Group V (H_2S preconditioned EXOs) (Fig.10f):

Widespread HO-1 positive cytoplasmic immunoreactivity was visualized in nearly all hepatocytes.

Morphometric results:

Mean number of homed PKH26 labelled NaHS preconditioned exosomes was significantly increased versus PKH26 labelled unconditioned exosomes **(Fig.4d)**.

The mean area percent of HMGB1 positive immunoreactivity **(Fig.8g)** of groups II (I/R group), III (Recovery group), and IV (H_2S + EXOs) recorded a significant rise while that of group V (H_2S preconditioned EXOs) showed non-significant increase versus group I (Control group). In comparison to group II, group III recorded a non-significant reduction, however groups IV as well as V revealed a significantly low value. Additionally, a significant diminution in group V versus group IV was demonstrated.

Nrf2 positive immunoreaction mean area percent **(Fig.9g)** of all studied groups illustrated a significant increase relative to control. Whereas a non-significant rise was illustrated in recovery group versus group II**.** Regarding groups IV & V, they recorded a significant rise in comparison to group II. Additionally, group V exhibited a significant elevation versus group IV.

Mean area percent of HO-1 positive immunoreactivity **(Fig.10g)** showed non-significant rise in group II as well as group III in comparison to control. Whereas, both groups IV and V illustrated a significant rise relative to the control and group II. Furthermore, a significant elevation in group V versus group IV was recorded.

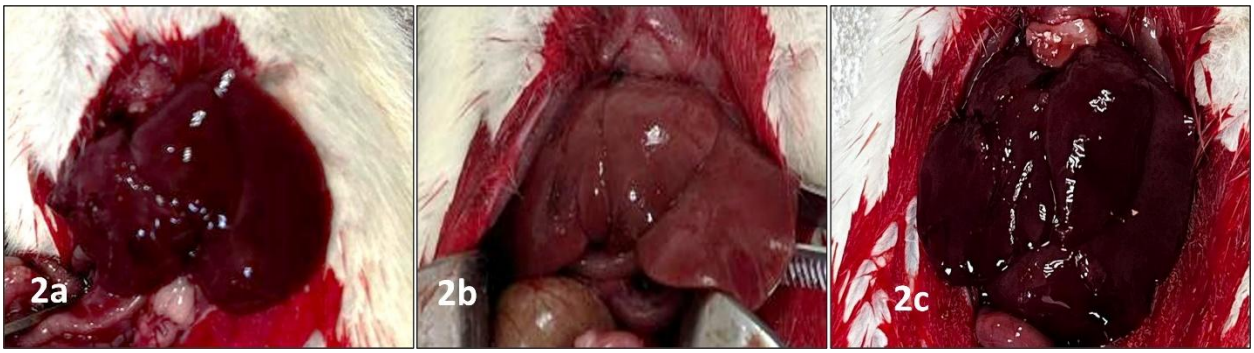

Figure 2: Macroscopic examination illustrating: **2a:** Before ischemia the liver surface shows no abnormalities **2b:** Following 30 minutes of ischemia, the liver appears pale. **2c:** Two hours after reperfusion, the liver surface becomes brown and congested.

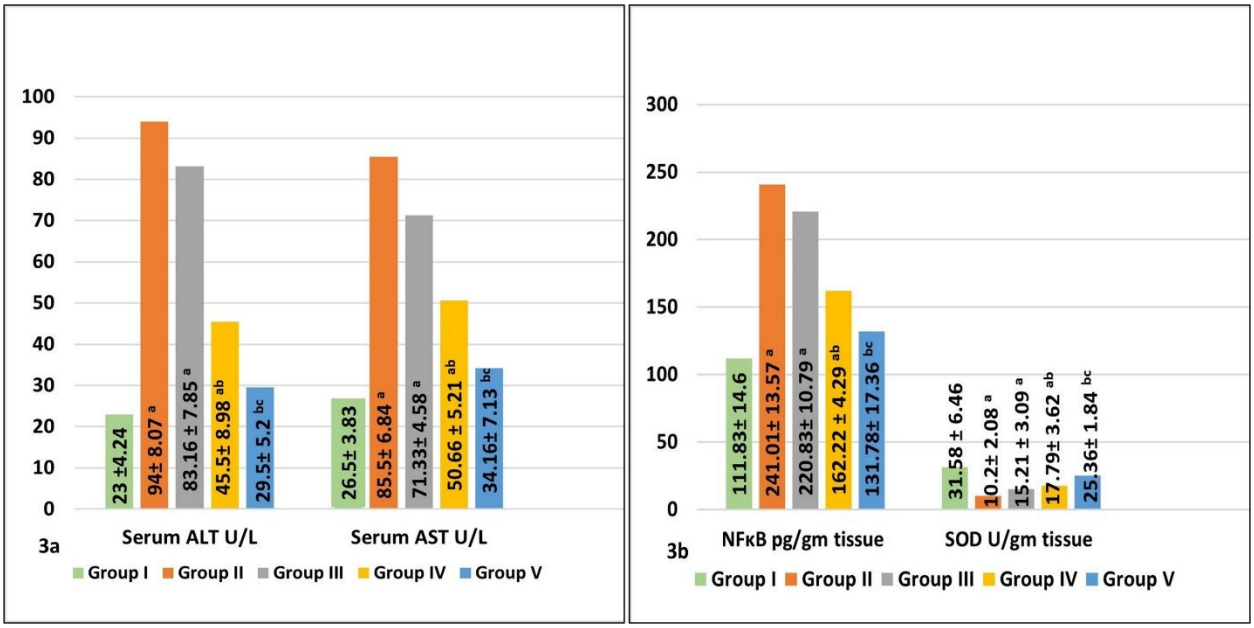

Figure 3: Demonstrating mean values of:

3a: Serum ALT and AST levels.

3b: Liver NF-κB and SOD levels.

[[a] as compared to control group, [b] as compared to group II & [c] as compared to group IV (significant difference at $P < 0.05$)]

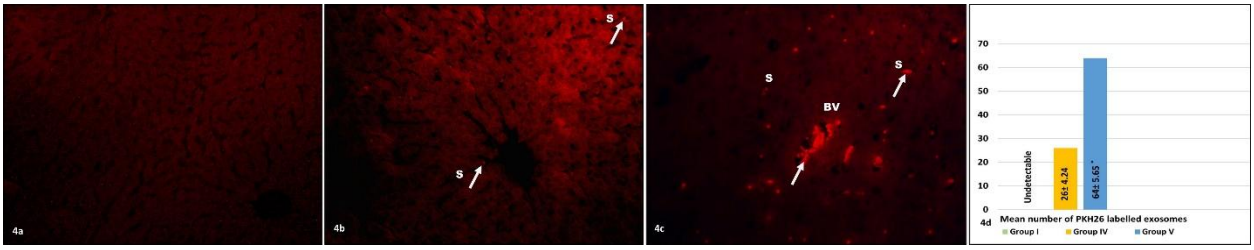

Figure 4: Fluorescent microscope photomicrographs of hepatic sections showing: **4a:** Group I (Negative control section) shows absence of red fluorescent of PKH26 dye in liver tissue **4b:** Group IV (H_2S + EXOs group) exhibits some labelled EXOs (arrows) in blood sinusoids (S) **4c:** Group V (H_2S preconditioned EXOs group), multiple labelled EXOs (arrows) are seen in hepatic blood vessels (BV) and blood sinusoids (S).

(PKH-26 fluorescent dye, x 400)

4d: Histogram: Illustrating mean number of PKH26 labelled EXOs: * as compared to unconditioned AMSCs-EXOs (significant difference at $P < 0.05$)

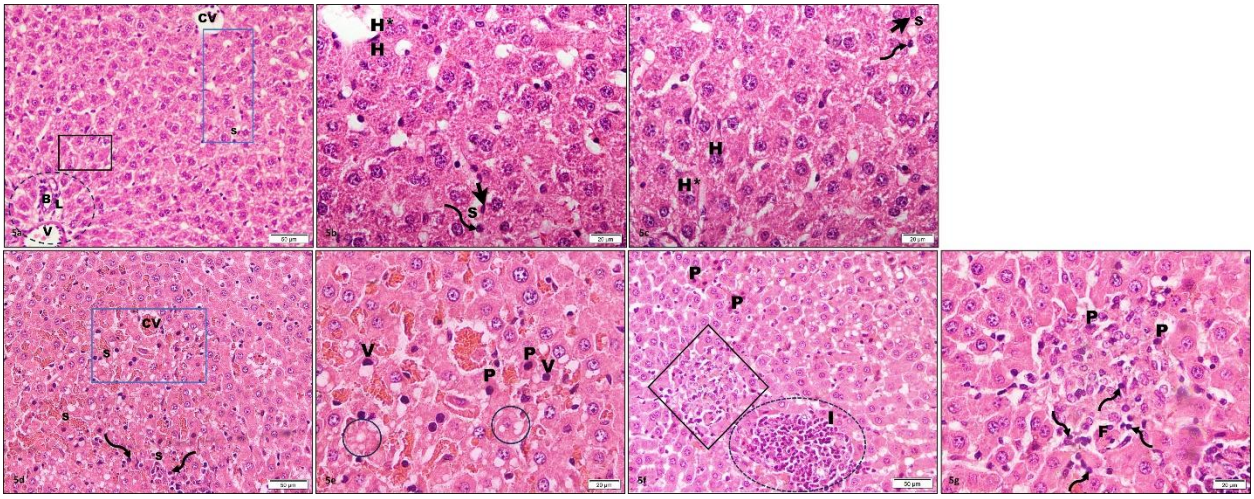

Figure 5: Light microscopic photomicrographs of liver section stained by H&E of:

Group I (Control group) (5a, 5b & 5c): 5a; Revealing hepatic cords radiating from the central vein (CV) toward the portal tract (dotted oval shape). The portal tract includes branch of portal vein (V), bile duct (B) & a lymphatic vessel (L). Blood sinusoids (S) are seen separating hepatic plates. **5b & 5c;** Higher magnification of the blue and black boxed parts in 5a showing areas of hepatocytes near the central vein & portal tract respectively. Hepatocytes (H) appear as polyhedral cells that exhibit central rounded vesicular nuclei with prominent nucleoli & acidophilic vacuolated cytoplasm. Some hepatocytes show binucleation (H*). Blood sinusoids (S) are lined by endothelial cells (short straight arrow) & Kupffer cells (wavy arrow)**.**

Group II (I/R group) (5d,5e,5f &5g): 5d; Illustrating markedly congested central vein (CV) & dilated congested sinusoids (S) with distorted hepatic cords. Many Kupffer cells can be noted (wavy arrows) among sinusoids (S). **5e;** Higher magnification of the blue boxed area in 5d illustrates pericentral hepatocytes. Some hepatocytes appear swollen with dark eccentric nuclei and large cytoplasmic vacuolations (V), others have deeply acidophilic cytoplasm with pyknotic nuclei (P). The circled areas exhibit disfigured hepatocytes with many cytoplasmic vacuolation. **5f;** Demonstrating recruitment of heavy inflammatory cell infiltration (I) around the portal tract (dotted oval shape). Note the focus of disorganized hepatocytes in the boxed area near the portal tract**.** Shrunken hepatocytes with deeply acidophilic cytoplasm and pyknotic nuclei are

encountered in upper part of field (P). **5g**; Higher magnification of boxed area in 5f reveals markedly disorganized hepatocytes surrounded by shrunken hepatocytes with deeply acidophilic cytoplasm & with either pyknotic (P) or fragmented nuclei (F). Kupffer cells are frequently noted among hepatocytes (wavy arrows).

(H&E, 5a,5d &5f x200, 5b, 5c, 5e & 5g x400)

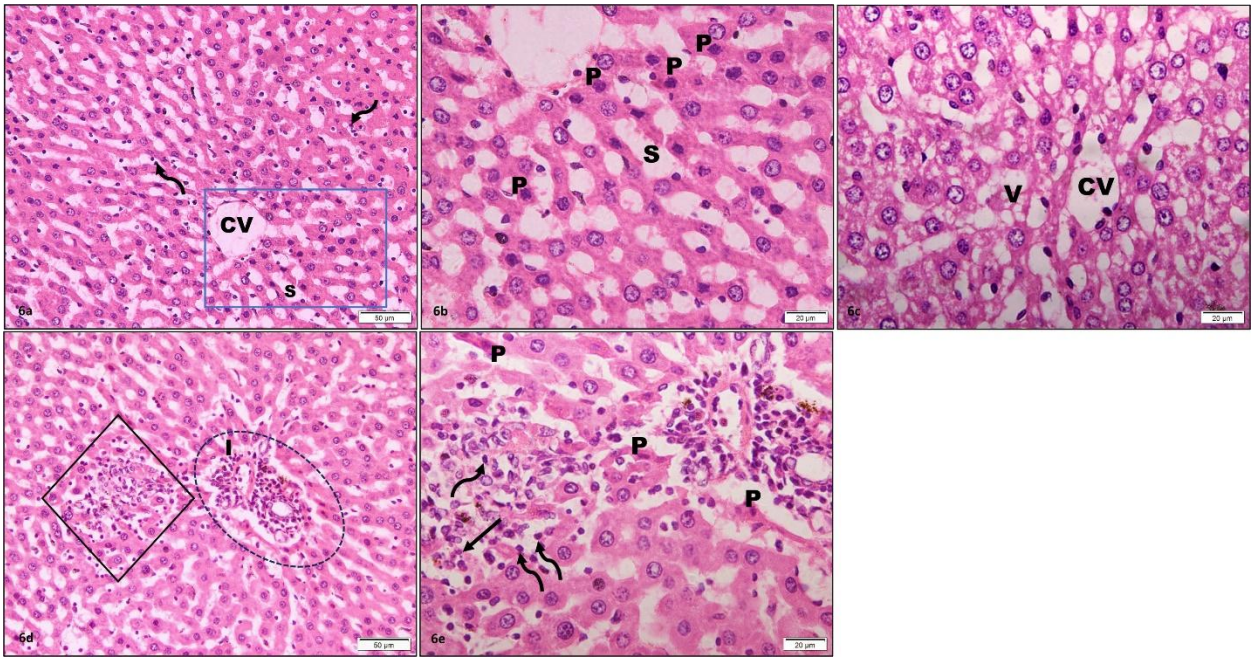

Figure 6: Light microscopic photomicrographs of H&E-stained hepatic sections of: **Group III (Recovery group) (6a,6b, 6c,6d &6e): 6a;** Revealing dilated central vein (CV) and dilated sinusoids (S). Note Kupffer cells inside blood sinusoids (wavy arrows). **6b;** Higher magnification of blue boxed area in 6a demonstrates dilated blood sinusoids (S) separating thin plates of hepatocytes. Some of the pericentral hepatocytes show deeply acidophilic cytoplasm with shrunken deeply stained irregular nuclei (P). **6c;** Another field showing hepatocytes with multiple cytoplasmic vacuolations (V) around central vein (CV). **6d;** Showing an area of deranged hepatocytes (boxed area) close to a focus of inflammatory cellular infiltration (I) around the portal tract (dotted oval shape). **6e;** Higher magnification of the boxed area in 6d shows acidophilic cytoplasmic remnants admixed with very small nuclear debris (long straight arrow). Kupffer cells are frequently noted (wavy arrows). Some

periportal hepatocytes appear shrunken with pyknotic nuclei and deeply acidophilic cytoplasm (P).

(H&E, 6a,6d x200, 6b,6c&6e x400)

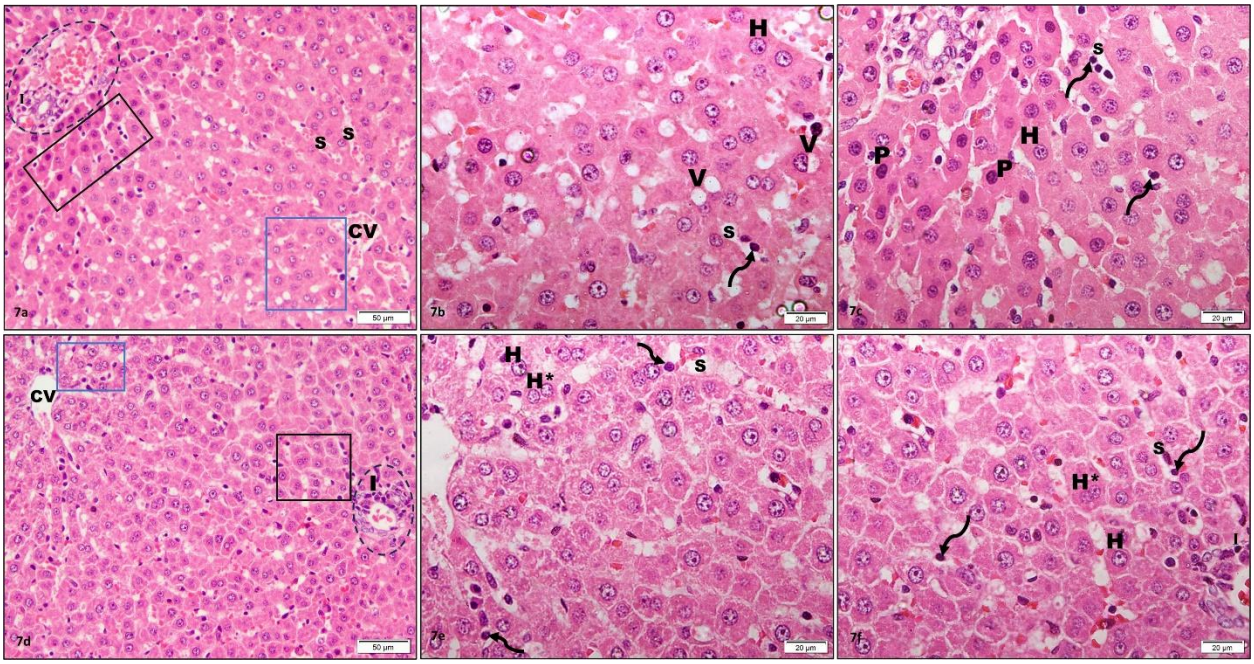

Figure 7: Light microscopic photomicrographs of a hepatic section stained with H&E of:

Group IV (H_2S + EXOs group) (7a,7b&7c): 7a; Demonstrating congested central vein (CV), some dilated congested sinusoids (S) and few inflammatory cells (I) around the congested portal tract vasculature (dotted oval shape). **7b & 7c;** Higher magnification of blue and black boxed parts in 7a showing area of hepatocytes near central vein and portal tract respectively. Hepatocytes (H) exhibit acidophilic cytoplasm with vesicular nuclei. Some pericentral hepatocytes show large cytoplasmic vacuolations (V). Moreover, periportal hepatocytes with pyknotic nuclei and deeply acidophilic cytoplasm (P) are seen. Kupffer cells are noted (wavy arrows) in sinusoids (S) in both **7b & 7c**.

Group V (H_2S preconditioned EXOs group) (7d,7e&7f): 7d; Illustrating apparently normal histological architecture of liver lobule. Hepatocytes plates are extending from the central vein (CV) toward the portal tract (dotted oval shape). Minimal inflammatory cells (I) are noted around the portal tract. **7e & 7f;** Higher magnifications of blue and black boxed parts in 7d showing areas of hepatocytes near central vein & portal tract respectively. Most liver cells (H) exhibit single central

rounded pale nuclei & acidophilic cytoplasm. While others are binucleated (H*). Note Kupffer cells (wavy arrows) inside blood sinusoids (S).

(H&E, 7a&7d x200, 7b, 7c,7e&7f x400)

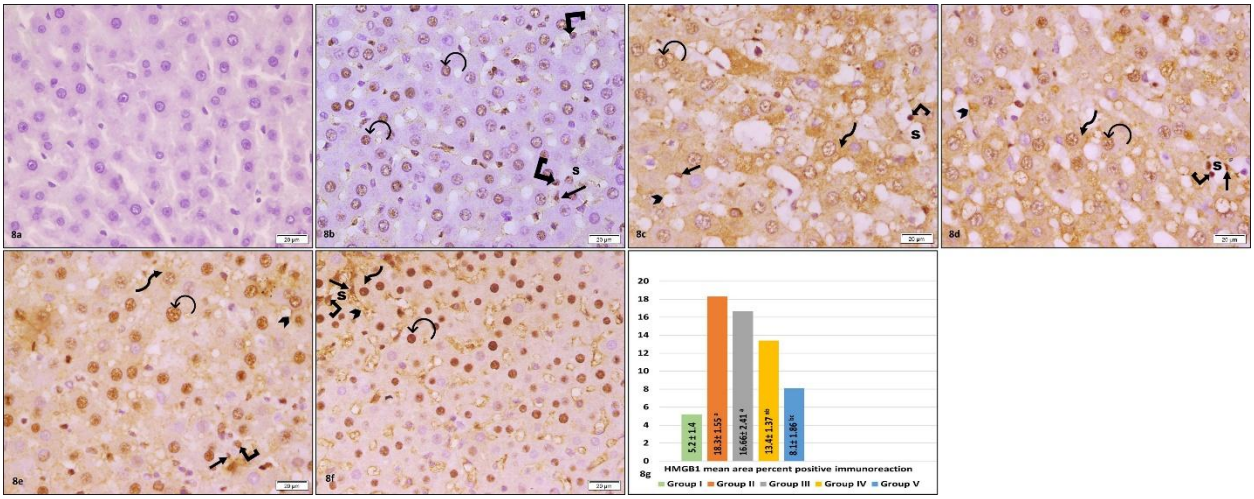

Figure 8: Light microscopic photomicrographs of HMGB1-stained liver sections of:

8a: <u>Negative control liver section</u> after skipping the HMGB1 primary antibody step illustrating negative immunostaining. **(x400)**

8b: Group I (Control group) showing positive nuclear immunoreaction in hepatocytes (curved arrows). Hepatic sinusoids (S) demonstrate positive nuclear immunoreaction in LSECs (straight arrow) and in Kupffer cells (right angled arrows).

8c: Group II (I/R group) demonstrating positive nuclear immunoreaction in some hepatocytes (curved arrow) as well as LSECs (straight arrow) and Kupffer cells (right angled arrow) lining the blood sinusoids (S). Note positive cytoplasmic immunoreaction in many hepatocytes (wavy arrow). In addition to the presence of cytoplasmic immunoreaction in LSECs (arrowhead).

8d: Group III (Recovery group) demonstrating positive cytoplasmic immunoreaction in many hepatocytes (wavy arrow). Positive cytoplasmic immunoreaction in LSECs (arrowhead) is also seen. In addition to the observed positive nuclear immunoreaction in multiple hepatocytes (curved arrow). Hepatic sinusoids (S) show positive nuclear immunoreaction in LSECs (straight arrow) and Kupffer cells (right angled arrow).

8e: Group IV (H_2S + EXOs group) demonstrating most of hepatocytes with positive nuclear immunoreactivity (curved arrow). Others have positive cytoplasmic immunoreactivity (wavy arrow)**.** Positive immunostaining in the nuclei (straight arrow) and cytoplasm (arrowhead) of LSECs is demonstrated. Note the positive nuclear immunoreaction in Kupffer cell (right angled arrow)**.**

8f: Group V (H_2S preconditioned EXOs group) demonstrating positive nuclear immunoreaction in multiple hepatocytes (curved arrow) & minimal cytoplasmic immunostaining in others (wavy arrow). Endothelial cells lining the blood sinusoids (S) show positive nuclear (straight arrow) and cytoplasmic (arrowhead) immunoreaction. In addition, positive nuclear immunoreaction in Kupffer cell (right angled arrow) was observed.

(anti HMGB1 immunohistochemical stain 8b, 8c, 8d, 8e &8f x400)

8g: Histogram illustrating the mean area percent of HMGB1 positive reaction. [^{a} as compared to control group, ^{b} as compared to group II & ^{c} as compared to group IV (significant difference at $P < 0.05$)]

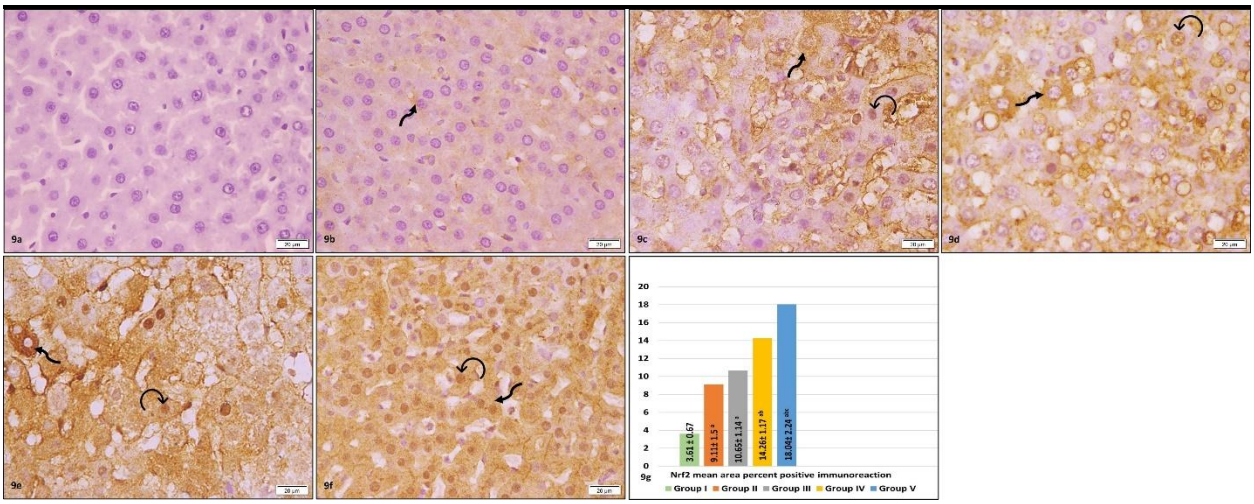

Figure 9: Light microscopic photomicrographs of Nrf2-stained liver sections of:

9a: Negative control liver section without adding the Nrf2 primary antibody illustrating negative immunoreactivity. **(x400)**

9b: Group I (Control group) demonstrating hepatocytes with positive cytoplasmic immunoreactivity (wavy arrow).

9c: Group II (I/R group) illustrating some hepatocytes with apparently increased positive cytoplasmic immunoreactivity to Nrf2 (wavy arrow) when compared to Fig. (9b) of group I. Note the Nrf2 positive nuclear immunoreactivity in a few hepatocytes (curved arrow).

9d: Group III (Recovery group) demonstrating some hepatocytes with positive cytoplasmic immunoreaction (wavy arrow). Note a few hepatocytes with positive nuclear immunoreaction (curved arrow).

9e: Group IV (H_2S + EXOs group) illustrating many hepatocytes with positive cytoplasmic immunostaining (wavy arrow). Also, there is positive nuclear immunostaining in some hepatocytes (curved arrow).

9f: Group V (H_2S preconditioned EXOs group) demonstrating widely distributed positive cytoplasmic (wavy arrow) and nuclear immunoreactivity (curved arrow) to Nrf2 in most hepatocytes.

(anti Nrf2 immunohistochemical stain 9b, 9c, 9d, 9e &9f x400)

9g: Histogram showing the mean area percent of Nrf2 positive reaction. [^{a} as compared to control group, ^{b} as compared to group II & ^{c} as compared to group IV (significant difference at $P < 0.05$)]

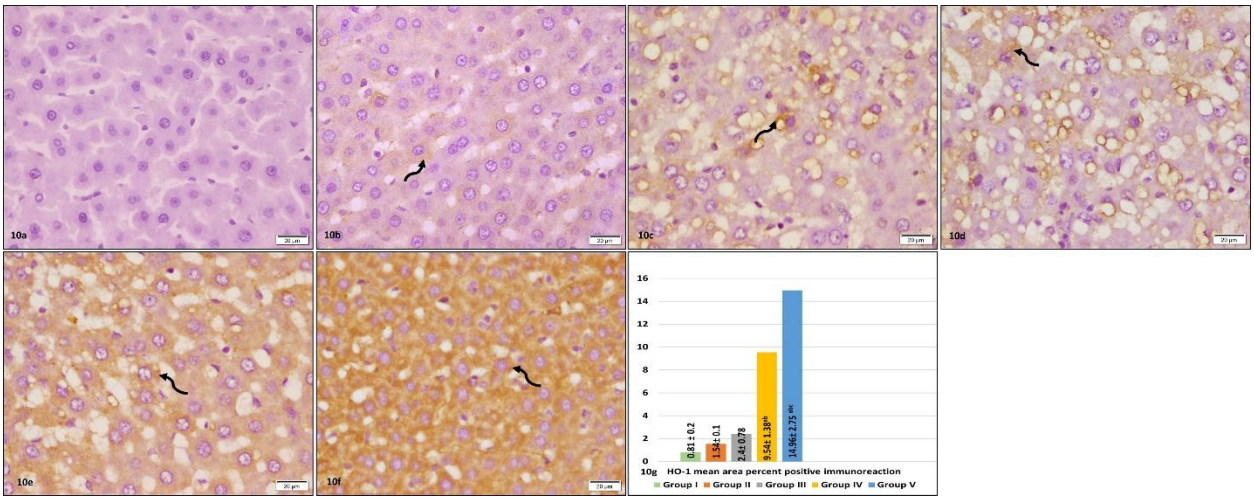

Figure 10: Light microscopic photomicrographs of HO-1-stained liver sections of:

10a: Negative control section of liver tissue without adding the HO-1 primary antibody showing negative immunoreaction. **(x400)**

10b: Group I (Control group) revealing few hepatocytes positive cytoplasmic immunoreaction (wavy arrow).

10c: Group II (I/R group) illustrating some hepatocytes with positive immunoreactivity in their cytoplasm (wavy arrow).

10d: Group III (Recovery group) showing positive cytoplasmic immunoreactivity in some liver cells (wavy arrow).

10e: Group IV (H_2S + EXOs group) showing most of hepatocytes with positive cytoplasmic immunoreaction (wavy arrow)**.**

10f: Group V (H_2S preconditioned EXOs group) showing nearly all hepatocytes with a widespread positive cytoplasmic immunoreactivity to HO-1 (wavy arrow)**.**

(anti HO-1 immunohistochemical stain 10b, 10c, 10d,10e&10f x400)

10g: Histogram demonstrating the mean area percent of HO-1 positive reaction. [^{a} as compared to control group, ^{b} as compared to group II & ^{c} as compared to group IV (significant difference at $P < 0.05$)]

4. Discussion:

Hepatic ischemia reperfusion injury (HIRI) is an inevitable outcome especially in partial liver resection and transplantation. It may lead to impaired recovery and poor prognosis of operative procedures. Therefore, management of HIRI is one of the most challenging problems associated with post-operative morbidity and mortality [43].

Total hepatic ischemia was induced in the present work because it perfectly imitates the clinical state of warm ischemia following Pringle maneuver. Pringle maneuver is used to minimize blood loss during liver resection and transplantation and is applied by blocking perfusion from hepatic artery along with portal vein to liver [44].

Hepatic ischemia more than 30 minutes leads to over 75% necrosis and severely affects liver function [45]. Such a massive injury is not similar to the clinical condition of liver surgery [46]. Therefore, 30 minutes only was chosen as a duration of ischemia in the present study.

The liver ischemia conducted was followed by 2 hours reperfusion according to study by [29] ***Czigany et al., 2019*** who found that the maximum of cellular injury was after 2 hours of hepatic reperfusion in rats, and was associated with significantly elevated AST, ALT, in addition to lactate dehydrogenase.

Male rats were chosen in the current research as HIRI was more serious in males than female patients [47]. This is linked to the variations in mitochondrial permeability transitions (MPT) between genders caused by estrogen hormone that can lead to variations in the intensity of calcium overload & I/R injury [48].

In the present work, the liver surface appeared pale after 30 minutes of ischemia due to obstructed liver blood supply, while after 2 hours of reperfusion, the liver surface appeared brown and congested. This coincided with the observation of ***Nakanuma et al., 2020*** [49].

Deaths recorded in the present study included two rats from group II (I/R group) and four rats from group III (Recovery group). This could be attributed to severe portal hypertension and progressive thrombosis in portal vein, hepatic artery, and caval veins induced by portal triad obstruction [50]. Vascular stasis and blood flow obstruction may also contribute to intracardiac and pulmonary thromboembolism [51].

In the same concern, in a former study HIRI rat didn't survive the planned 6 hours [52] and

24 hours of reperfusion [53]. Congestion of great splanchnic vein during clamping procedure of portal triad [52] results in destruction of intestinal barrier followed by endotoxin/bacterial translocation to portal blood aggravating liver injury, and eventually liver failure and death occurs [53].

Being indicators of liver cell damage [54], serum level of liver enzymes (ALT & AST) was analyzed in the current study and recorded significant elevation in group II (I/R group) indicating a decline in liver function following HIRI. These results were similarly recorded in a former study [55]. The elevated level of liver enzymes could be explained by disruption of the hepatocytes' membrane, necrosis and cellular damage that resulted in leakage of liver enzymes into the blood [45].

Liver ischemia reperfusion injury comprises multiple series of events such as mitochondrial dysfunction, acidosis, calcium overload, oxidative stress after ischemia. Following reoxygenation, more ROS production and upregulation of proinflammatory cytokine was encountered [56, 57]. Such diversity of events is linked to the pathophysiology of the I/R, thus achieving effective protection might not be targeted by a single mechanism to reduce I/R injury [58].

NF-κB has a central role as a transcriptional regulator in response to cellular stress. The pathologic process of HIRI is tightly linked to the NF-κB pathway, blocking this pathway may delay inflammatory reaction, oxidative stress, as well as cellular death [59, 60]. In the current study, I/R group demonstrated significant rise in tissue NF-κB versus control group.

Superoxide dismutase (SOD) possesses a selective effect in protection against oxidative stress in the body. Therefore, the enzyme is a useful therapeutic measure for diseases caused by reactive oxygen species [61]. In this study, tissue SOD was significantly reduced in I/R group relative to control.

H&E-stained hepatic sections of I/R group revealed hepatocytes with deeply acidophilic cytoplasm in addition to shrunken deeply stained nuclei, indicating apoptosis. While other hepatocytes showed features of necrosis such as cell swelling, disfigurement, and cytoplasmic vacuolation. Apoptosis as well as necrosis are both modes of cellular death that caused distortion of hepatic cords and hepatic lobular architecture. In harmony with our findings, similar histological alterations were illustrated in HIRI models [55,62].

The pericentral area in I/R group demonstrated markedly congested central vein along with dilated congested sinusoids that were surrounded by either apoptotic or necrotic hepatocytes. These results are consistent with [49] ***Nakanuma et al., 2020*** who mentioned that sinusoidal affection occurred mostly in zone III causing hepatic parenchyma injury and congestion in the pericentral area. The researchers related the vascular congestion to endothelial cell injury and lost fenestrations. Moreover, they attributed the increased apoptotic hepatocytes in zone III to the relatively poor oxygen nature of zone III that becomes more hypoxic after hepatic ischemia.

Aiming to explain the cellular damage in hepatic parenchyma, it could be suggested that hypoxic then hyperoxic injuries following I/R injury results in cell swelling, necrotic cell degeneration and apoptosis, endothelial dysfunction, activation of both Kupffer cells and neutrophils, and local inflammatory reactions inducing cytokine storm that damages cellular structures and results in cell death [63, 64].

The affection of hepatocytes in group II was not only observed in the pericentral zone (Zone III) but also was noticed in periportal zone (Zone I), together with heavy inflammatory infiltration around portal tract. This is in line with other researchers who reported bridging necrosis in HIRI models [65, 66]. The bridging necrosis is linked to increased pro-inflammatory mediator HMGB1 release from affected hepatocytes which attach to Toll like receptor 4 (TLR4, HMGB1 receptor) on neighboring hepatocytes resulting in necrosis of neighboring hepatocytes [67].

Additionally, Kupffer cells were frequently seen in both pericentral and periportal areas. This might be related to phagocytic role of Kupffer cells as a trial to preserve liver homeostasis. Also, they coordinate the inflammatory process by monocytes and neutrophils recruitment to area of injury [26, 68]. Neutrophils release free radicals and subsequently consumption of antioxidants as SOD and glutathione (GSH). This cascade exaggerates the inflammatory response that eventually results in hepatocytes death by necrosis and apoptosis leading to organ dysfunction [69].

Dead cells release damage-associated molecular patterns (DAMPs), like ROS, nuclear proteins, DNA fragments in addition to cytosolic proteins [70]. HMGB1 is a crucial endogenous DAMP that rises noticeably in the early stages of ischemia [71]. HMGB1 acts as a proinflammatory mediator

and may be secreted by phagocytes, endothelial along with necrotic cells [72,73,74]. Regarding HMGB1 immuno-stained sections of group II, some hepatocytes demonstrated HMGB1 positive cytoplasmic immunoreactivity, while others showed nuclear immunoreactivity, indicating HMGB1 translocation from nucleus to cytoplasm. A similar record following 3 hours of liver intoxication model [75] was noticed. HMGB1 is mostly found in the nucleus, under different stressful conditions it can translocate from nucleus to cytoplasm. Translocation of HMGB1 indicates that it has been activated [76]. Statistically HMGB1 positive immunostaining mean area percent, likewise tissue NF-κB mean value showed a significant rise in group II versus control. Going along with the former findings, a significant elevation in levels of TLR4, HMGB1 in addition to NF-κB assessed by immunoblotting were similarly noted after HIRI [77]. Since necrotic or injured hepatocytes released HMGB1 [78], HMGB1 can activate Kupffer cells via binding to TLR-4 [68]. The stimulated Kupffer cells release ROS [79] along with pro-inflammatory cytokines via TLR-4/ NF-κB pathway [80]. TLR-4 phosphorylates as well as activate NF-κB transcription factor, which upregulates secretion of proinflammatory cytokine [81]. This could explain the recorded increase in NF-κB level. Nuclear factor erythroid 2-related factor 2 (Nrf2), a transcriptional factor, stimulates several antioxidant genes to defense against ROS [5].

Examination of Nrf2 immunostained hepatic sections of group II revealed some hepatocytes with positive cytoplasmic immunoreactivity and few hepatocytes with nuclear immunoreactivity. This indicates transfer of Nrf2 from cytoplasm to nucleus, which was backed by significant elevation in Nrf2 mean area percent versus group I. Such result was hand in hand with renal I/R injury model [82]. Furthermore, this was similarly recorded using Western blot in mouse models of HIRI [12, 83]. The increased Nrf2 immunoreactivity might be attributed to I/R injury that stimulates Nrf2 dissociation from its negative regulator Keap1, causing nuclear translocation of Nrf2, attaching to antioxidant response element (ARE) [84,85] and activating target genes of antioxidant enzymes [HO-1, peroxidase-1, SOD, GSH] along with detoxification enzymes [mainly glutathione-S-transferase, and NAD(P)H quinone dehydrogenase 1 (NQO1)] to eliminate ROS and reduce the redox reaction [86].

To assess the Nrf2/HO-1/SOD pathway, HO-1 expression using immunohistochemical staining and the tissue level of SOD using colorimetric method were examined. A non-significant rise in HO-1 positive immunoreactivity and a significant low level of SOD was detected in group II versus group I. The preceding findings are similarly reported where a minimal rise in HO-1 immunostaining and a significant decrease in tissue SOD level were shown in HIRI group [83]. These might be explained by failure of hepatocytes to achieve completed stimulation of Nrf2/HO-1/SOD pathway thereby affecting promotion of ARE response leading to SOD depletion. This was similarly mentioned where elevated free radicles exceeded the power of hepatocytes to remove them, resulting in reduced antioxidant enzymes such as catalase (CAT) as well as GSH [87].

Similar to group II, group III (Recovery group) illustrated significant deterioration in serum ALT, AST, tissue NF-κB and SOD levels along with HMGB1, Nrf2, and HO-1 immunoreactivity versus control group. These results agree with another research that reported significant increase in ALT, AST, tissue malondialdehyde (MDA), also a significant drop in SOD, glutathione peroxidase levels one day of reperfusion in HIRI rats as compared to sham rats. Likewise, there were necrotic hepatocytes and vascular congestion [88]. I/R injury is a multifactorial where hepatic inflammation may continue up to a week after reperfusion [89]. This could support the persistent hepatocyte affection, inflammatory response and oxidative state reported in group III of the present work.

On the other hand, group III recorded a slight improvement that was statistically non-significant in all previously mentioned findings as compared to group II. As well as histologically, there was reduced congestion. These results can be explained by improvement in the microcirculation and tissue oxygen saturation of liver tissue after 24 hours reperfusion versus 2 hours reperfusion [29]. Better microcirculation led to a decrease in ischemia reperfusion damage [29,90,91].

By comparing group IV (H_2S + EXOs) and group V (H_2S preconditioned EXOs) AMSCs proliferation, total protein concentration in exosomes and number of homed PKH26 labelled exosomes were significantly increased in group V versus group IV. This indicates that H_2S precondition enhances in vitro AMSCs proliferation, exosome protein production

and incorporation of exosomes into the injured tissue.

This was formerly reported where NaHS treated bone marrow mononuclear cells showed elevated cell proliferation, homing, and migration [92]. In addition, another study exhibited a minor increase in the protein concentration of NaHS preconditioned EXOs relative to that of unconditioned EXOs [93]. This could be attributed to the effect of H_2S that changes the protein profile of exosomes and activates their uptake by target cells [94].

Both groups IV and V ameliorated all biochemical alterations (they decreased ALT, AST, NF-κB and increased SOD) and H&E findings (hepatocytes necrosis, apoptosis, inflammation and congestion) that were recorded in group II. However, group V illustrated superior results when compared to group IV.

Concerning group IV (H_2S + EXOs), the effect of H_2S administration was similarly recorded where an improvement of liver enzymes, hepatocytes vacuolar degeneration, necrosis, apoptosis and inflammatory cell infiltration were demonstrated [95]. This could be explained by H_2S ability to preserve mitochondrial integrity and drop in mitochondrial ROS production, hence improve I/R injury in myocardium [96]. The reported H_2S anti-inflammatory along with anti-oxidative stress effects could support the significant reduction in NF-κB and rise in SOD detected in the current work.

As regards the impact of MSCs-EXOs administration, similar results were noted such as decreased liver enzymes, inflammatory cytokines and apoptosis [97]. It was also found that MSCs-EXOs administration alleviated sinusoidal congestion, inflammatory cell infiltration, cell death and improved levels of SOD, glutathione peroxidase (GSH-Px), and MDA [98]. Exosomes promote cell-to-cell communication, by transferring proteins (like adhesion molecules, signal transduction proteins, heat-shock proteins, and cytoplasmic enzymes) in addition to microRNAs between cells [99]. Also, MSCs-EXOs can limit tissue injury, alter immune responses, and enhance tissue repair [100].

Despite the enormous impact of exosomes, multiple limitations are documented [101]. Initially, a lower number of exosomes obtained under conventional culture of MSCs [102]. Additionally, the trial to increase their generations by multiple culturing of MSCs causes MSCs senescence and subsequently reduces therapeutic influence of their exosomes [103]. Thus, the therapeutic effect of MSC-EXOs is closely linked to

their cellular condition [104]. Recent studies have shown that modulation of MSCs culture conditions or pretreatment are adaptive targets to enhance yield and therapeutic efficiency of MSCs-EXOs [101]. Hydrogen sulfide regulates different cellular pathways. It participates and controls biological processes of cell survival/death, proliferation/hypertrophy, differentiation, metabolism, oxidative stress, and inflammation [105]. Therefore, EXOs of H_2S-pretreated MSCs were examined in current research.

Regarding group V (H_2S preconditioned EXOs), ALT, AST, NF-κB, SOD, and H&E findings were almost comparable to control. Similarly, reduction of ALT, AST, and attenuation of sinusoidal congestion, hepatocytes death were detected following treatment with H_2S preconditioned EXOs [93]. Hand in hand with results of renal I/R study, preconditioned MSCs with H_2S showed increased efficacy of EXOs in restoring renal function, reduced polymerase chain reaction (PCR) expression of NF-κB & increased SOD enzymatic activity [26]. Moreover, other researchers proved that extracellular vesicles of H_2S-pretreated MSCs exerted a stronger protective effect on ischemic brain model compared to that of untreated MSCs [106]. The authors concluded that was through a specific release of factors which target cells and lower inflammatory response.

Immunohistochemically, groups IV and V in the present work exhibited improvement in HMGB1, Nrf2 and HO-1 results compared to group II.

According to group IV (H_2S + EXOs), HMGB1 immuno-stained liver sections recorded positive immunostaining in nuclei of most hepatocytes as well as cytoplasm of others. Statistically a significant reduction in HMGB1 positive immunoreactivity mean area percent and consequently decrease in tissue NF-κB level was recorded versus group II, indicating inhibition of HMGB1/NF-κB pathway (inflammatory pathway). This agrees with previous research that illustrated a decrease in HMGB1 immunoreactivity in lung following NaHS treatment of hemorrhagic shock model [107]. Going with the previously mentioned results, similar observations were noticed in colitis model using western blot analysis [108]. It was suggested that H_2S antioxidant effect decreases ROS and cell death, which in turn lowers the release of HMGB1. This results in decline of Kupffer cell activation, release of inflammatory mediators and cellular damage [96].

It was also found that the treatment with MSC-EXOs suppressed HMGB1 and NF-κB expressions using western blot and ELISA respectively in a lung injury model [109]. An assumption of the anti-inflammatory mechanism of MSCs-EXOs was mediated by prevention of cytoplasmic translocation of nuclear HMGB1 through deacetylation [110]. Besides the repression of NF- κB phosphorylation thus preventing activation as well as translocation of NF-κB as shown in renal I/R model [111].

As regard the upregulation of Nrf2/HO-1/SOD pathway (antioxidant pathway) in the current study, a rise in Nrf2 positive cytoplasmic & nuclear immunoreaction as well as an increase in HO-1 positive cytoplasmic immunoreactivity were demonstrated in group IV in comparison to I/R group. This was statistically emphasized by a significant elevation in their mean area percent along with the significant rise in value of tissue SOD level versus group II.

Other studies linked such upregulation to H_2S which enhances disassociation of Keap1/Nrf2 through S-sulfhydration of Keap1 (negative regulator of Nrf2), thus increases Nrf2 nuclear localization and subsequent activation of antioxidant defense [112,113]. Moreover, NaHS treated renal I/R rats exhibited reduced MDA, increased SOD, and decreased apoptotic cells suggesting that NaHS provides a cytoprotective effect against oxidative stress through maintaining the intracellular antioxidant enzymes [114]. Additionally, ADMSCs-EXOs was assumed to inhibit Keap1 and enhance Nrf2 expression and nucleus translocation, thus increase HO-1 expression [115].

Comparing rats treated with H_2S preconditioned EXOs in group V with rats treated by H_2S + EXOs in group IV, a more pronounced effect concerning the immunohistochemical expression of all markers was detected in group V. This was confirmed by the significant decrease of HMGB1 immunoreaction that was localized in nuclei of multiple hepatocytes, indicating that HMGB1 was not activated. Additionally, the mean value of tissue NF-κB demonstrated a significant diminution versus group IV. Whereas, immuno-histochemical staining for Nrf2 revealed a widely distributed positive cytoplasmic and nuclear immunoreactivity and for HO-1, a widespread positive cytoplasmic immunoreactivity was detected nearly in all hepatocytes. These findings indicate potentiated upregulation of Nrf2/HO-1 pathway which were confirmed morphometrically by significantly increased

mean area percent of Nrf2 and HO-1 positive immunoreactivity and biochemically by significant elevation of mean value of tissue SOD level in group V compared to group IV. Similar findings were obtained by previous researchers who recorded that H_2S preconditioned exosomes reduced PCR expression of NF-κB along with its downstream of interleukins, IL-1α, IL-6, IL-12, & tumor necrotic factor-α (TNF-α) thus inhibition of inflammatory response [26]. The authors also reported decreased MDA level as well as increased western blot expression of Nrf2 and enzymatic activity of SOD, glutathione S-transferase (GST) & glutathione peroxidase (GPx) relative to the untreated EXOs in renal I/R. This is in line with former study where NaHS preconditioning MSCs-EXOs reduced total oxidant status, phosphorylation of NF-κB in addition to inflammatory mediators like TNF-α & IL-6 in HIRI [93]. The better amelioration of the previously mentioned biochemical and histological alterations in group V than IV of the current work could be attributed to the increased exosome protein concentration as well as the increased number of exosomes homing in the liver tissue thus alleviating HIRI.

5. Conclusion:

It is possible to conclude that H_2S + EXOs group and H_2S preconditioned EXOs group protected the liver against pathological alterations induced by HIRI. Their protective effects appeared via their anti-inflammatory impact through repression of HMGB1/NF-kB signaling pathway as well as anti-oxidative effect through stimulation of Nrf2/HO-1/SOD pathway that was accompanied by decreased oxidative stress and thus decreased cell damage. However, the use of H_2S preconditioned EXOs showed better regenerative effect in rats indicating that H_2S preconditioning may be considered after further research as a promising goal for enhancement of exosome properties for management of acute liver injury especially during liver surgery.

Recommendation

Further studies are recommended to examine and compare the treatment application before and after surgical procedures. More investigations are needed to clarify the mechanism of H_2S preconditioning regulating exosome proteins content, identify the protein types affected by H_2S. In addition to how H_2S enhances the incorporation of preconditioned exosomes into injured liver than unconditioned exosomes. Also, the pivotal role of Von-

Kupffer cells in the pathogenesis of HIRI could be thoroughly studied.

Conflict of interests:

There are no conflicts of interest.

6. References:

1- Elbaset M.A., Arafa E.S.A., Sherbiny G.A.E., Bakky M.S.A., Elgendy A.N.A.M., Quercetin modulates iNOS: eNOS and NOSTRIN expressions and attenuates oxidative stress in warm hepatic ischemia-reperfusion injury in rats, Beni-Suef Univ. J. Basic Appl. Sci.2015; 4: 246–255.

2- Ali JM, Davies SE, Brais RJ, Randle LV, Klinck JR, Allison ME, Chen Y, Pasea L, Harper SF, Pettigrew GJ. Analysis of ischemia/reperfusion injury in time-zero biopsies predicts liver allograft outcomes. Liver Transpl. 2015; 21:487-499.

3- Yamada N, Karasawa T, Wakiya T, Sadatomo A, Ito H, Kamata R, Watanabe S, Komada T, Kimura H, Sanada Y, Sakuma Y, Mizuta K, Ohno N, Sata N, Takahashi M. Iron overload as a risk factor for hepatic ischemia-reperfusion injury in liver transplantation: Potential role of ferroptosis. American Journal of Transplantation.2020; 20:1606-1618.

4- Guan Y, Yao W, Yi K, Zheng C, Lv S, Tao Y, Hei Z, Li M. Nanotheranostics for the Management of Hepatic Ischemia-Reperfusion Injury. Small. 2021;17: e2007727.

5- Bardallo RG, Panisello-Roselló A, Sanchez-Nuno S, Alva N, Roselló-Catafau J, Carbonell T. Nrf2 and oxidative stress in liver ischemia/reperfusion injury. The FEBS journal; 2022; 289: 5463–5479.

6- Liu Y, Yang L, Tao K, Vizcaychipi MP, Lloyd DM, Sun X, Irwin MG, Ma D, Yu W. Protective effects of hydrogen enriched saline on liver ischemia reperfusion injury by reducing oxidative stress and HMGB1 release. BMC Gastroenterol. 2014; 14:12.

7- Yang X, Yao W, Shi H, Liu H, Li Y, Gao Y, Liu R, Xu L. Paeoniflorin protects Schwann cells against high glucose induced oxidative injury by activating Nrf2/ARE pathway and inhibiting apoptosis. J Ethnopharmacol. 2016; 185:361–369

8- Krajka-Kuźniak V, Paluszczak J, Baer-Dubowska W. The Nrf2-ARE signaling pathway: An update on its regulation and possible role in cancer prevention

and treatment. Pharmacol Rep. 2017; 69:393-402.

9- Ahmed SMU, Luo L, Namani A, Wang XJ, Tang X. Nrf2 signaling pathway: pivotal roles in inflammation. Elsevier. 2017; 1863:585–97.

10- Raghunath A, Sundarraj K, Nagarajan R, Arfuso F, Bian J, Kumar AP, Sethi G, Perumal E. Antioxidant response elements: Discovery, classes, regulation and potential applications. Redox Biol. 2018; 17:297–314.

11- Bao L, Li J, Zha D, Zhang L, Gao P, Yao T, Wu X. Chlorogenic acid prevents diabetic nephropathy by inhibiting oxidative stress and inflammation through modulation of the Nrf2/HO-1 and NF-kB pathways. Int Immunopharmacol.2018; 54:245–253

12- Zhou Y, Tan Z, Huang H, Zeng Y, Chen S, Wei J, Huang G, Qian C, Yuan G, He S. Baicalein pre- treatment alleviates hepatic ischemia/reperfusion injury in mice by regulating the Nrf2/ARE pathway. Experimental and Therapeutic Medicine.2021; 22: 1-9.

13- Bai Y, Han YD, Yan XL, Ren J, Zeng Q, Li XD, Pei XT, Han Y: Adipose mesenchymal stem cell-derived exosomes stimulated by hydrogen peroxide enhanced skin flap recovery in ischemia-reperfusion injury. Biochem Biophys Res Commun.2018; 500: 310-317.

14- Zhang Y, Han F, Gu L, Ji P, Yang X, Liu M, Tao K, Hu D: Adipose mesenchymal stem cell exosomes promote wound healing through accelerated keratinocyte migration and proliferation by activating the AKT/HIF-1α axis. J Mol Histol.2020; 51: 375-383.

15- Kugeratski FG, Kalluri R: Exosomes as mediators of immune regulation and immunotherapy in cancer. FEBS J.2021; 288: 10-35.

16- Gnecchi M, Danieli P, Malpasso G, Ciuffreda MC. Paracrine mechanisms of mesenchymal stem cells in tissue repair. Methods Mol Biol. 2016; 1416:123.

17- Rager TM, Olson JK, Zhou Y. Wang Y, Besner GE. Exosomes secreted from bone marrow-derived mesenchymal stem cells protect the intestines from experimental necrotizing enterocolitis. J Pediatr Surg. 2016; 51:942–947.

18- Gurunathan S, Kang M-H, Jeyaraj M, Qasim M, Kim J-H. Review of the Isolation, Characterization, Biological Function, and Multifarious Therapeutic

Approaches of Exosomes. Cells. 2019; 8:307.

19- Ocansey DKW, Pei B, Yan Y, Qian H, Zhang X, Xu W, Mao F. Improved therapeutics of modified mesenchymal stem cells: an update. J Transl Med. 2020; 18:42.

20- Hu C, Li L. Preconditioning influences mesenchymal stem cell properties in vitro and in vivo. J Cell Mol Med. 2018; 22:1428-1442.

21- Xiao Q, Ying J, Xiang L, Zhang C. The biologic effect of hydrogen sulfide and its function in various diseases. Medicine. 2018; 97: e13065.

22- Zheng J, Zhao T, Yuan Y, Hu N, Tang X. Hydrogen sulfide (H2S) attenuates uranium-induced acute nephrotoxicity through oxidative stress and inflammatory response via Nrf2-NF-kappa B pathways. Chem. Biol. Interact.2015; 242: 353–362.

23- Zhang Q, Liu S, Li T, Yuan L, Liu H, Wang X, Wang F, Wang S, Hao A, Liu D, Wang Z. Preconditioning of bone marrow mesenchymal stem cells with hydrogen sulfide improves their therapeutic potential. Oncotarget. 2016; 7:58089-58104.

24- Azarbarz N, Seifabadi ZS, Moaiedi MZ, Mansouri E. Assessment of the effect of sodium hydrogen sulfide (hydrogen sulfide donor) on cisplatin-induced testicular toxicity in rats. Environmental Science and Pollution Research.2020; 27:8119-8128

25- Yuan O, Lin C, Wagner J, Anderson J, Archard J, Deng P, Halmai J, Bauer G, Fink K, Fury B, Perotti N, Walker J, Pollock K, Apperson M, Butters J, Belafsky P, Farwell D, Kuhn M, Nolta J, Anderson J. Exosomes Derived from Human Primed Mesenchymal Stem Cells Induce Mitosis and Potentiate Growth Factor Secretion. Stem Cells and Development. 2019; 28: 398-409.

26- Wang Y, Wang R, Li Z, Wang X, Qiao X, Ma T, Jiang Z, Huang L. H2S treatment improves protective effect of MSC-derived exosomes upon of renal ischemia/reperfusion fibrosis by suppressing inflammatory signaling of TGF-β and NF-kB as well as ROS generation. Archives of Medical Science.2021;1-36.

27- Ibrahim MA, Abdelzaher WY, Ibrahim YF, Ahmed AF, Welson NN, Al-Rashed S, Batiha GE, Abdel-Aziz AM. Diacerein protects rats with liver ischemia/reperfusion damage: Down-regulation of TLR4/ NFκ-B signaling

pathway. Biomed Pharmacother. 2020; 134: 111063.

28- Chen L, Ma K, Fan H, Wang X, Cao T. Exogenous hydrogen sulfide protects against hepatic ischemia/reperfusion injury by inhibiting endoplasmic reticulum stress and cell apoptosis. Experimental and Therapeutic Medicine.2021; 22: 1-7

29- Czigany Z, Hata K, Lai W, Schwandt T, Yamamoto Y, Uemoto S, Tolba R. A Dual Protective Effect of Intestinal Remote Ischemic Conditioning in a Rat Model of Total Hepatic Ischemia. Journal of Clinical Medicine 2019; 8: 1-16.

30- Zhang Y, Li Y, Wang Q, Zheng D, Feng X, Zhao W, Cai L, Zhang Q, Xu H, Fu H. Attenuation of hepatic ischemia- reperfusion injury by adipose stem cell- derived exosome treatment via ERK1/2 and GSK- 3β signaling pathways. Int J Mol Med. 2022; 49:13.

31- González-Cubero E, González-Fernández ML, Gutiérrez-Velasco L, Navarro-Ramírez E, Villar-Suárez V. Isolation and characterization of exosomes from adipose tissue-derived mesenchymal stem cells. J Anat. 2021; 238: 1203-1217.

32- Willis GR, Fernandez-Gonzalez A, Anastas J, Vitali SH, Liu X, Ericsson M, Kwong A, Mitsialis SA, Kourembanas S. Mesenchymal Stromal Cell Exosomes Ameliorate Experimental Bronchopulmonary Dysplasia and Restore Lung Function through Macrophage Immunomodulation. Am J Respir Crit Care Med.2018; 197: 104-116.

33- Hajian R, DeCastro J, Parkinson J, Kane A, Camelo AFR, Chou PP, Yang J, Wong N, Hernandez EDO, Goldsmith B, Conboy I, Aran K. Rapid and electronic identification and quantification of age-specific circulating exosomes via biologically activated graphene transistors. Advanced Biology.2021; 5: 2000594

34- Zou W, Yang Y, Gu Y, Zhu P, Zhang M, Cheng Z, Liu X, Yu Y, Peng X. Repeated Blood Collection from Tail Vein of Non-Anesthetized Rats with a Vacuum Blood Collection System. Journal of visualised experiment 2017; 130: 1-6**.**

35- Lima NKS, Farias WRA, Cirilo MAS, Oliveira AG, Farias JS, Aires RS, Muzi-Filho H, Paixão ADO, Vieira LD. Renal ischemia-reperfusion leads to hypertension and changes in proximal

tubule Na+ transport and renin-angiotensin-aldosterone system: Role of NADPH oxidase. Life Sci. 2021; 266:118879

36- Kükner A, Soyler G, Toros P, Dede G, Meriçli F, Işık S, Edebal O, Özoğul C. Protective effect of Coriandrum sativum extract against inflammation and apoptosis in liver ischemia /reperfusion injury. Folia Morphologica.2021; 80: 363-371

37- Yücel A, Aydogan M, Ucar M, Sarıcı K, Karaaslan M. Effects of Apocynin on Liver Ischemia-Reperfusion Injury in Rats. Transplantation Proceedings.2019; 51: 1180-1183

38- Suvarna K, Layton C, Bancroft J. The haematoxylins and eosin Connective and mesenchymal tissue with their stains & Immunohistochemical and immunofluorescent techniques. In Bancroft's Theory and Practice of Histological Techniques (Eighth Edition), Elsevier, 2019, pp: 126-138, 153-175 & 337-394

39- Dong L, Chen F, Xu M, Yao L, Zhang Y, Zhuang Y. Quercetin attenuates myocardial ischemia-reperfusion injury via downregulation of the HMGB1-TLR4-NF-κB signaling pathway. American journal of translation research.2018; 10: 1273–1283.

40- Yu K, Zhang J, Cao Z, Ji Q, Han Y, Song M, Shao B, Li Y. Lycopene attenuates AFB1-induced renal injury with the activation of the Nrf2 antioxidant signaling pathway in mice. Food and Function.2018; 9: 6427-6434.

41- Zhang A, Suzuki T, Adachi S, Naganuma E, Suzuki N, Hosoya T, Itoh K, Sporn MB, Yamamoto M. Distinct Regulations of HO-1 Gene Expression for Stress Response and Substrate Induction. Mol Cell Biol.2021; 41 :0023621

42- Emsley R, Dunn G, White IR. Mediation and moderation of treatment effects in randomized controlled trials of complex interventions. Statistical Methods in Medical Research.2010; 19: 237-270

43- Ito Y, Hosono K, Amano H. Responses of hepatic sinusoidal cells to liver ischemia-reperfusion injury. Front Cell Dev Biol.2023; 11:1171317.

44- Piardi T, Lhuaire M, Memeo R, Pessaux P, Kianmanesh R, Sommacale D. Laparoscopic Pringle maneuver: how we do it? Hepatobiliary Surg Nutr.2016; 5: 345-349.

45- Mard SA, Akbari G, Dianat M, Mansouri E. Protective effects of crocin and zinc sulfate on hepatic ischemia-reperfusion injury in rats: a comparative experimental model study. Biomed Pharmacother.2017; 96:48–55.

46- Olthof PB, van Golen RF, Meijer B, van Beek AA, Bennink RJ, Verheij J, van Gulik TM, Heger M. Warm ischemia time-dependent variation in liver damage, inflammation, and function in hepatic ischemia/reperfusion injury. Biochim Biophys Acta Mol Basis Dis.2017; 1863: 375-385.

47- Li Z, Lu S, Qian B, Meng Z, Zhou Y, Chen D, Chen B, Yang G, Ma Y. Sex differences in hepatic ischemia–reperfusion injury: a cross-sectional study. Sci Rep.2023; 13: 5724.

48- Fels JA, Manfredi G. Sex differences in ischemia/reperfusion injury: The role of mitochondrial permeability transition. Neurochem.2019; 44: 2336–2345.

49- Nakanuma S, Tajima H, Takamura H, Sakai S, Gabata R, Okazaki M, Shinbashi H, Ohbatake Y, Makino I, Hayashi H, Miyashita T, Fushida S, Ohta T. Pretreatment with a Phosphodiesterase-3 Inhibitor, Milrinone, Reduces Hepatic Ischemia-Reperfusion Injury, Minimizing Pericentral Zone-Based Liver and Small Intestinal Injury in Rats. Ann Transplant.2020; 25: 922306.

50- Kolovrat M, Gojkovic S, Krezic I, Malekinusic D, Vrdoljak B, Kasnik Kovac K, Kralj T, Drmic D, Barisic I, Horvat Pavlov K, Petrovic A, Duzel A, Knezevic M, Mirkovic I, Kokot A, Boban Blagaic A, Seiwerth S, Sikiric P. Pentadecapeptide BPC 157 resolves Pringle maneuver in rats, both ischemia and reperfusion. World J Hepatol. 2020;12: 184-206.

51- Vetrugno L, Cherchi V, Lorenzin D, De Lorenzo F, Ventin M, Zanini V, Terrosu G, Risaliti A, Baccarani U, Bove T. The Challenging Management of an Intracardiac Thrombus in a Liver Transplant Patient at the Reperfusion Phase: A Case Report and Brief Literature Review. Transplant Direct.2021; 7: 746.

52- Gomes HM, Serigiolle LC, Rodrigues DA, Lopes CM, Studart Sdo V, Leme PL. Unfeasible experimental model of normothermic hepatic ischemia and reperfusion in rats using the Pringle maneuver. Arq Bras Cir Dig. 2014;27: 196-200.

53- Liu B, Ma ZY, Wu G, Qian JM. Butyrate protects rats from hepatic

ischemia/reperfusion injury. Int J Clin Exp Med. 2015,8: 5406-5413.

54- Chinnappan R, Mir TA, Alsalameh S, Makhzoum T, Adeeb S, Al-Kattan K, Yaqinuddin A. Aptasensors Are Conjectured as Promising ALT and AST Diagnostic Tools for the Early Diagnosis of Acute Liver Injury. Life.2023; 13: 1273.

55- Morsy MA, Abdel-Gaber SA, Rifaai RA, Mohammed MM, Nair AB, Abdelzaher WY. Protective mechanisms of telmisartan against hepatic ischemia/reperfusion injury in rats may involve PPARγ-induced TLR4/NF-κB suppression. Biomed Pharmacother.2021; 145: 112374.

56- van Alem CMA, Boonstra M, Prins J, Bezhaeva T, van Essen MF, Ruben JM, Vahrmeijer AL, van der Veer EP, de Fijter JW, Reinders ME, Meijer O, Metselaar JM, van Kooten C, Rotmans JI. Local delivery of liposomal prednisolone leads to an anti-inflammatory profile in renal ischaemia-reperfusion injury in the rat. Nephrol Dial Transplant. 2018; 33:44–53.

57- Teodoro JS, Varela AT, Duarte FV, Gomes AP, Palmeira CM, Rolo AP. Indirubin and NAD (+) prevent mitochondrial ischaemia/reperfusion damage in fatty livers. Eur J Clin Invest. 2018; 48: e12932.

58- Toyoda T, Tosaka S, Tosaka R, Maekawa T, Cho S, Eguchi S, Nakashima M, Sumikawa K. Milrinone-induced postconditioning reduces hepatic ischemia-reperfusion injury in rats: the roles of phosphatidylinositol 3-kinase and nitric oxide. J Surg Res. 2014; 186:446-51.

59- Mitchell JP, Carmody RJ. NF-κB and the Transcriptional Control of Inflammation. Int Rev Cell Mol Biol.2018; 335:41-84.

60- Awad AS, Elariny HA, Sallam AS. Colchicine attenuates renal ischemia-reperfusion-induced liver damage: implication of TLR4/NF-κB, TGF-β, and BAX and Bcl-2 gene expression. Can J Physiol Pharmacol. 2022; 100:12–18.

61- Younus H. Therapeutic potentials of superoxide dismutase. Int J Health Sci (Qassim).2018; 12: 88-93.

62- Uylaş MU, Şahin A, Şahintürk V, Alataş İÖ. Quercetin dose affects the fate of hepatic ischemia and reperfusion injury in rats: an experimental research. Int J Surg.2018; 53: 117-121.

63- Guan LY, Fu PY, Li PD, Li ZN, Liu HY, Xin MG, Li W. Mechanisms of hepatic ischemia-reperfusion injury and protective effects of nitric oxide. World J Gastrointest Surg.2014; 6: 122-128.

64- Bhatraju P, Crawford J, Hall M, Lang JD Jr. Inhaled nitric oxide: Current clinical concepts. Nitric Oxide.2015; 50: 114-128.

65- Abdel-Wahab AF, AL-Harizy WM. Propofol Protects against Ischemia/Reperfusion Injury Associated with Reduced Apoptosis in Rat Liver. International Scholarly Research Notices.2013; 2013: 1-8.

66- Al Mograмpi S, Boumpoureka C, Afaloniati H, Lagou M, Angelopoulou K, Anestakis D, Tampouratzi ZG, Iliadis S, Antoniadis N, Giakoustidis A, Papalois A, Papadopoulos V, Poutahidis T, Giakoustidis D. Inhibition of γδ-TcR or IL17a Reduces T-Cell and Neutrophil Infiltration after Ischemia/Reperfusion Injury in Mouse Liver. J Clin Med. 2023;12: 1751

67- Minsart C, Liefferinckx C, Lemmers A, Dressen C, Quertinmont E, Leclercq I, Devière J, Moreau R, Gustot T. New insights in acetaminophen toxicity: HMGB1 contributes by itself to amplify hepatocyte necrosis in vitro through the TLR4-TRIF-RIPK3 axis. Sci Rep.2020; 10: 5557.

68- Dong X, Liu J, Xu Y, Cao H. Role of macrophages in experimental liver injury and repair in mice. Exp Ther Med.2019;17: 3835-3847.

69- Tan Z, Jiang R, Wang X, Wang Y, Lu L, Liu Q, Zheng SG, Sun B, Ryffel B. RORγt+IL-17+ neutrophils play a critical role in hepatic ischemia-reperfusion injury. J Mol Cell Biol.2013; 5:143-146.

70- Hirao H, Nakamura K, Kupiec-Weglinski JW. Liver ischemia-reperfusion injury: a new understanding of the role of innate immunity. Nat Rev Gastroenterol Hepatol.2022; 19: 239-256.

71- Lu TF, Yang TH, Zhong CP, Shen C, Lin WW, Gu GX, Xia Q, Xu N. Dual Effect of Hepatic Macrophages on Liver Ischemia and Reperfusion Injury during Liver Transplantation. Immune Netw.2018;18: 24.

72- Lotze MT, Tracey KJ. High-mobility group box 1 protein (HMGB1): nuclear weapon in the immune arsenal. Nat Rev Immunol.2005; 5: 331-342.

73- Williams CD, Bajt ML, Sharpe MR, McGill MR, Farhood A, Jaeschke H. Neutrophil activation during

acetaminophen hepatotoxicity and repair in mice and humans. Toxicol Appl Pharmacol.2014; 275: 122-133.

74- Huebener P, Pradere JP, Hernandez C, Gwak GY, Caviglia JM, Mu X, Loike JD, Schwabe RF. The HMGB1/RAGE axis triggers neutrophil-mediated injury amplification following necrosis. J Clin Invest.2015;125: 539-50.

75- Zhou RR, Zhao SS, Zou MX, Zhang P, Zhang BX, Dai XH, Li N, Liu HB, Wang H, Fan XG. HMGB1 cytoplasmic translocation in patients with acute liver failure. BMC Gastroenterol.2011; 11: 21.

76- Sun R, Sun S, Zhang Y, Zhou Y, Shan Y, Li X, Fang W. PCV2 Induces Reactive Oxygen Species to Promote Nucleocytoplasmic Translocation of the Viral DNA Binding Protein HMGB1 To Enhance Its Replication. J Virol 2020; 94: e00238-20.

77- Koh WU, Kim J, Lee J, Song G-W, Hwang GS, Tak E, Song J-G. Remote Ischemic Preconditioning and Diazoxide Protect from Hepatic Ischemic Reperfusion Injury by Inhibiting HMGB1-Induced TLR4/MyD88/NF-κB Signaling. Int. J. Mol. Sci.2019; 20: 5899

78- Kuramochi M, Izawa T, Pervin M, Bondoc A, Kuwamura M, Yamate J. The kinetics of damage-associated molecular patterns (DAMPs) and toll-like receptors during thioacetamide-induced acute liver injury in rats. Exp Toxicol Pathol.2016; 68: 471-477.

79- Nastos C, Kalimeris K, Papoutsidakis N, Tasoulis MK, Lykoudis PM, Theodoraki K, Nastou D, Smyrniotis V, Arkadopoulos N. Global consequences of liver ischemia/reperfusion injury. Oxid Med Cell Longev.2014; 2014: 906965.

80- Wang L, Li N, Lin D, Zang Y. Curcumin protects against hepatic ischemia/reperfusion induced injury through inhibiting TLR4/NF-κB pathway. Oncotarget.2017; 8: 65414-65420.

81- Mahmoud MF, Gamal S, El-Fayoumi HM. Limonin attenuates hepatocellular injury following liver ischemia and reperfusion in rats via toll-like receptor dependent pathway. Eur J Pharmacol.2014; 740: 676–682.

82- Zheng Y, Lu H, Huang H. Desflurane Preconditioning Protects Against Renal Ischemia-Reperfusion Injury and Inhibits Inflammation and Oxidative Stress in Rats Through Regulating

the Nrf2-Keap1-ARE Signaling Pathway. Drug Des Devel Ther.2020; 14: 1351-1362.

83- Chen Y, Li T, Tan P, Shi H, Cheng Y, Cai T, Bai J, Du Y, Fu W. Kaempferol from Penthorum chinense Pursh Attenuates Hepatic Ischemia/Reperfusion Injury by Suppressing Oxidative Stress and Inflammation Through Activation of the Nrf2/HO-1 Signaling Pathway. Front Pharmacol.2022; 13: 857015.

84- Galicia-Moreno M, Lucano-Landeros S, Monroy-Ramirez HC, Silva-Gomez J, Gutierrez-Cuevas J, Santos A, Armendariz-Borunda J. Roles of Nrf2 in Liver Diseases: Molecular, Pharmacological, and Epigenetic Aspects. Antioxidants (Basel).2020; 9: 980.

85- Jayasuriya R, Dhamodharan U, Ali D, Ganesan K, Xu B, Ramkumar K M. Targeting Nrf2/Keap1 Signaling Pathway by Bioactive Natural Agents: Possible Therapeutic Strategy to Combat Liver Disease. Phytomedicine.2021; 92: 153755.

86- Xue R, Qiu J, Wei S, Liu M, Wang Q, Wang P, Sha B, Wang H, Shi Y, Zhou J, Rao J, Lu L. Lycopene alleviates hepatic ischemia reperfusion injury via the Nrf2/HO-1 pathway mediated NLRP3 inflammasome inhibition in Kupffer cells. Ann Transl Med.2021; 9: 631.

87- Elias-Miró M, Jiménez-Castro MB, Rodés J, Peralta C. Current knowledge on oxidative stress in hepatic ischemia/reperfusion. Free Radic Res.2013; 47: 555-568.

88- Shi Y, Qiu X, Dai M, Zhang X, Jin G. Hyperoside Attenuates Hepatic Ischemia-Reperfusion Injury by Suppressing Oxidative Stress and Inhibiting Apoptosis in Rats. Transplant Proc. 2019;51: 2051-2059.

89- Datta G, Fuller BJ, Davidson BR. Molecular Mechanisms of Liver Ischemia Reperfusion Injury: Insights from Transgenic Knockout Models. World J. Gastroenterol.2013; 19:1683–1698.

90- Kraemer R, Lorenzen J, Kabbani M, Herold C, Busche M, Vogt PM, Knobloch K. Acute effects of remote ischemic preconditioning on cutaneous microcirculation—A controlled prospective cohort study. BMC Surg.2011; 11: 32.

91- Szijarto A, Czigany Z, Turoczi Z, Harsanyi L. Remote ischemic preconditioning—A simple, low-risk

method to decrease ischemic reperfusion injury: Models, protocols and mechanistic background. A review. J. Surg. Res.2012; 178: 797–806.

92- Khanna A, Indracanti N, Chakrabarti R, Indraganti PK. Short-term ex-vivo exposure to hydrogen sulfide enhances murine hematopoietic stem and progenitor cell migration, homing, and proliferation. Cell Adh Migr. 2020; 14: 214-226.

93- Sameri MJ, Savari F, Hoseinynejad K, Danyaei A, Mard SA. The hepato-protective effect of H2S-modified and non-modified mesenchymal stem cell exosomes on liver ischemia-reperfusion injury in mice: The role of MALAT1. Biochem Biophys Res Commun. 2022; 635: 194-202.

94- Zhou Y-K, Han C-S, Zhu Z-L, Chen P, Wang Y-M, Lin S, Chen L-J, Zhuang Z-M, Zhou Y-H, Yang R-L. M2 exosomes modified by hydrogen sulfide promoted bone regeneration by moesin mediated endocytosis. Bioactive Materials. 2024; 31: 192–205.

95- Ruan Z, Liang M, Deng X, Lai M, Shang L, Su X. Exogenous hydrogen sulfide protects fatty liver against ischemia-reperfusion injury by regulating endoplasmic reticulum stress-induced autophagy in macrophage through mediating the class A scavenger receptor pathway in rats. Cell Biol Int. 2019; 44: 306-316.

96- Andreadou I, Schulz R, Papapetropoulos A, Turan B, Ytrehus K, Ferdinandy P, Daiber A, Di Lisa F. The role of mitochondrial reactive oxygen species, NO and H_2 S in ischaemia/reperfusion injury and cardioprotection. J Cell Mol Med.2020; 24: 6510-6522.

97- Xie K, Liu L, Chen J, Liu F. Exosomes derived from human umbilical cord blood mesenchymal stem cells improve hepatic ischemia reperfusion injury via delivering miR-1246. Cell Cycle. 2019; 18: 3491-3501.

98- Nong K, Wang W, Niu X, Hu B, Ma C, Bai Y, Wu B, Wang Y, Ai K. Hepatoprotective effect of exosomes from human-induced pluripotent stem cell-derived mesenchymal stromal cells against hepatic ischemia-reperfusion injury in rats. Cytotherapy. 2016; 18:1548-1559.

99- Schorey JS, Bhatnagar S. Exosome function: from tumor immunology to pathogen biology. Traffic. 2008; 9: 871-881.

100- Liang X, Ding Y, Zhang Y, Tse HF, Lian Q. Paracrine mechanisms of mesenchymal stem cell-based therapy: current status and perspectives. Cell Transplant. 2014; 23:1045-1059.

101- Phan J, Kumar P, Hao D, Gao K, Farmer D, Wang A. Engineering mesenchymal stem cells to improve their exosome efficacy and yield for cell-free therapy. J Extracell Vesicles. 2018; 7: 1522236.

102- Madrigal M, Rao KS, Riordan NH. A review of therapeutic effects of mesenchymal stem cell secretions and induction of secretory modification by different culture methods. J Transl Med. 2014; 12: 260.

103- Joo HS, Suh JH, Lee HJ, Bang ES, Lee JM. Current knowledge and Future Perspectives on Mesenchymal Stem Cell-Derived Exosomes as a New Therapeutic Agent. Int J Mol Sci. 2020; 21: 727.

104- Wang J, Bonacquisti EE, Brown AD, Nguyen J. Boosting the Biogenesis and Secretion of Mesenchymal Stem Cell-Derived Exosomes. Cells. 2020; 9: 660.

105- Zhang D, Du J, Tang C, Huang Y, Jin H. H_2S-induced sulfhydration: Biological function and Detection Methodology. Front. Pharmacol. 2017; 8: 608.

106- Chu X, Liu D, Li T, Ke H, Xin D, Wang S, Cao Y, Xue H, Wang Z. Hydrogen sulfide-modified extracellular vesicles from mesenchymal stem cells for treatment of hypoxic-ischemic brain injury. J Control Release. 2020; 328: 13-27.

107- Xu DQ, Gao C, Niu W, Li Y, Wang YX, Gao CJ, Ding Q, Yao LN, Chai W, Li ZC. Sodium hydrosulfide alleviates lung inflammation and cell apoptosis following resuscitated hemorrhagic shock in rats. Acta Pharmacol Sin. 2013; 34:1515-1525.

108- Török S, Almási N, Valkusz Z, Pósa A, Varga C, Kupai K. Investigation of H_2S Donor Treatment on Neutrophil Extracellular Traps in Experimental Colitis. Int J Mol Sci. 2021; 22: 12729.

109- Xu B, Gan CX, Chen SS, Li JQ, Liu MZ, Guo GH. BMSC-derived exosomes alleviate smoke inhalation lung injury through blockade of the HMGB1/NF-κB pathway. Life Sci. 2020; 257:118042.

110- Wei W, Guo X, Gu L, Jia J, Yang M, Yuan W, Rong S. Bone marrow mesenchymal stem cell exosomes suppress phosphate-induced aortic

calcification via SIRT6-HMGB1 deacetylation. Stem Cell Res Ther. 2021; 12: 235.

111- Li L, Wang R, Jia Y, Rong R, Xu M, Zhu T. Exosomes Derived From Mesenchymal Stem Cells Ameliorate Renal Ischemic-Reperfusion Injury Through Inhibiting Inflammation and Cell Apoptosis. Front Med (Lausanne). 2019; 6: 269.

112- Guo C, Liang F, Shah MW, Yan X. Hydrogen sulfide protected gastric epithelial cell from ischemia/reperfusion injury by Keap1 s-sulfhydration, MAPK dependent anti-apoptosis and NF-kappaB dependent anti-inflammation pathway. Eur. J. Pharmacol. 2014; 725: 70–78.

113- Zhao S, Song T, Gu Y, Zhang Y, Cao S, Miao Q, Zhang X, Chen H, Gao Y, Zhang L, Han Y, Wang H, Pu J, Xie L, Ji Y. Hydrogen Sulfide Alleviates Liver Injury Through the S-Sulfhydrated-Kelch-Like ECH-Associated Protein 1/Nuclear Erythroid 2-Related Factor 2/Low-Density Lipoprotein Receptor-Related Protein 1 Pathway. Hepatology. 2020; 73: 282-302.

114- Choi EK, Park SH, Lim JA, Hong SW, Kwak KH, Park SS, Lim DG, Jung H. Beneficial Role of Hydrogen Sulfide in Renal Ischemia Reperfusion Injury in Rats. Yonsei Med J.2018; 59: 960-967.

115- Shen K, Jia Y, Wang X, Zhang J, Liu K, Wang J, Cai W, Li J, Li S, Zhao M, Wang Y, Hu D. Exosomes from adipose-derived stem cells alleviate the inflammation and oxidative stress via regulating Nrf2/HO-1 axis in macrophages. Free Radic Biol Med. 2021; 165: 54-66.